Lava flow hazard modelling during the 2021 Fagradalsfjall eruption, Iceland: Applications of MrLavaLoba

Gro B. M. Pedersen[1], Melissa A. Pfeffer[2], Sara Barsotti[2], Simone Tarquini[3], Mattia de´ Michieli Vitturi[3,4], Bergrún A. Óladóttir[1,2], Ragnar Heiðar Þrastarson[2]

[1]Nordic Volcanological Center, Institute of Earth Sciences, University of Iceland, Reykjavík, 102, Iceland
[2]Icelandic Meteorological Office, Reykjavík, 105, Iceland
[3]Istituto Nazionale di Geofisica e Vulcanologia, Pisa, 56127, Italy
[4]Department of Geology, University at Buffalo, Buffalo, New York 14260, USA

Correspondence to: Gro B. M. Pedersen (gro@hi.is)

Abstract

On March 19, 2021, the first eruption on the Reykjanes Peninsula in ca. 800 years took place in Fagradalsfjall ~~on the Reykjanes Peninsula~~, in the backyard of the capital Reykjavík. This 6-month long effusive eruption ~~was~~ is the most visited eruption in Iceland to date and needed intense lava flow hazard assessment. ~~and~~It became a ~~test~~ case study for hazard assessment for future eruptions on the Peninsula, which ~~can~~have the potential to issue lava into inhabited areas or inundate essential infrastructure.

In this study we documented how lava flow modelling strategies were implemented using the stochastic code MrLavaLoba, to ~~evaluating~~ evaluate hazards during ~~the 6-month long~~this effusive event. Overall, the purposes were three-fold~~:~~: (a) Pre-eruption simulations to investigate potential lava inundation of critical infrastructure ~~at danger for lava flow inundation~~, (b) Syn-eruptive simulations for short-term (two weeks~~'~~ time ~~frame) lava flow hazard assessment and (c) Syn-eruptive simulations for long-term (months to years) hazard assessments ~~(months to years)~~. ~~Furthermore~~Additionally, strategies for lava barrier testing were developed and ~~incorporation of near-real time~~ syn-eruptive topographic models were incorporated into simulations in near-real time~~were implemented~~.

During the crisis the code was updated to increase ~~functionalites~~functionalities such as considering multiple active vents. Post-eruption, the~~as well as~~ code was optimiz~~edation that led to a~~ substantially decrease~~ing in~~ the computational time required for the simulations, speeding up the delivery of final products.

Formatted: Superscript

Formatted: Not Highlight

Formatted: Not Highlight

Formatted: Not Highlight

Formatted: Not Highlight

1 Introduction

On March 19, 2021, the first eruption on the Reykjanes Peninsula in ca. 800 years started at Mt. Fagradalsfjall, a mountainous area cut by nested enclosed valleys (Fig. 1). Being located in the backyard of the capital Reykjavík and the international airport, this eruption was the most visited eruption in Iceland to date.~~On March 19, 2021, an eruption started at Mt. Fagradalsfjall on the Reykjanes Peninsula, Iceland, a mountainous area cut by nested enclosed valleys (Fig. 1). Being the first eruption on Reykjanes Peninsula in ca. 800 years and being located in the backyard of the capital Reykjavík and the international airport, this eruption was the most visited eruption in Iceland to date.~~ Thousands of people visited the eruption each day~~It was easily accessible to the 2/3 of the Icelandic population as well as international tourists, and was visited by thousands of tourists per day.,~~ which therefore ~~and hence the eruption~~ needed intense monitoring and thorough hazard assessment (Barsotti et al., ~~in review~~2023). ~~Luckily, t~~The 2021 Fagradalsfjall eruption did not impact any critical infrastructure. However, it became a case study for the monitoring and hazard assessment for future effusive eruptions since~~However, since~~ several volcanic systems on the Reykjanes peninsula have the potential to issue lava into inhabited areas or inundate critical infrastructure~~, the eruption became a test case for the monitoring and hazard assessment for future eruptions in the area that can be more destructive~~.

In this study we document how various lava flow modelling strategies using the stochastic ~~stochastic~~ code MrLavaLoba (de' Michieli Vitturi and Tarquini, 2018) were implemented during the pre-eruptive unrest phase and during the eruption~~. .~~ ~~Th~~The code ~~code~~ proved to be a useful and a flexible tool to evaluate pre-eruption as well as syn-eruptive short-term and long-term hazards during the 6-month long effusive event ~~during the 6-month long effusive event~~. ~~Changes in~~ Different approaches as well as new developments of the code were used to account for the changes in the eruptive behavior, and to resolve challenges provided by the complex topographic terrain, where infilling and overflowing of nested valleys created time-evolving hazards for visitors. ~~Furthermore~~Additionally, strategies for lava barrier testing were developed and near-real time syn-eruptive topographic models were incorporated as the eruption progressed. ~~In spite of recent technological progresses, the so-called "deterministic" lava flow models tackling the physics of the lava emplacement provide only simplified solutions (e.g., the vertical structure of lava flows is typically not considered), at the cost of greater complexity and greater computational requirements. For this reason, we preferred to use the stochastic model MrLavaloba because it accounts for the lava flow volume and modify the topography during the simulated lava emplacement. In this work~~We describe in detail the model performance throughout the eruption and at the end we address caveats that should be considered when applying the code and make suggestions for future improvements. ~~we also address caveats that should be considered when applying the code and make suggestions for future improvements to the MrLavaLoba code.~~

Formatted: Font color: Auto

1.1. Lava flow simulations

Numerical ~~L~~lava flow modelling codes ~~is a well-known tool to anticipate~~for the simulation of lava flow emplacement

and lava flow models are commonwidely used for hazard and risk assessments before and during eruptions. Existing lava flow models are often divided into deterministic codes and probabilistic stochastic (or stochastic probabilistic) codes. The dDeterministic codes are intended to mimic the behavior of the natural systems by calculatingmodeling physical processes based on a suite of physical propertiesa set of conservation equations (e.g., Dietterich et al., 2017, FLOWGO: Harris and Rowland, 2001, PyFLOWGO: Chevrel et al., 2018, MAGFLOW: Cappello et al., 2016a). Stochastic codes capture that lava is a gravitational flowLava which flows tends to follow the steepest path of descent downhill (Favalli et al., 2012), but they doit can deviate from it in a probabilistichaotic way , which is captured by stochastic codes (e.g., DOWNFLOW: Favalli et al., 2005, Tarquini and Favalli, 2013, Q-LAVHA: Mossoux et al., 2016). Recent developments of stochastic probabilistic codes have included erupted volume as an input parameter allowing the thickness of lava field thickness to be one of the estimated model result (Glaze and Baloga, 2013, MrLavaLoba: de' Michieli Vitturi and Tarquini 2018). The deterministic codes and some of the stochastic probabilistic ones attempt to replicate the patterns of channelized lava flows (e.g., Mossoux et al., 2016, Diettrich et al., 2017, Chevrel et al., 2018), while a few stochastic probabilistic codes additionally replicate tube-fed flows (Favalli et al., 2005, de' Michieli Vitturi and Tarquini, 2018). The probabilistic code "MrLavaLoba" can also account for the erupted volume and the syn-eruptive modification of the topography (de' Michieli Vitturi and Tarquini, 2018).

Starting with the pioneering work at Mt. Etna during the 1991-93 eruption (Barberi and Villari, 1994), the numerical modeling of lava flows has increasingly been increasingly used to mitigate thepotential destruction that can be caused by active lava flows. This approach has been refined over the years in both theoretical and practical asrespects (e.g., Wright et al., 2008, Cappello et al., 2016a, Harris et al., 2019). including using an operational tool which combines satellite-derived discharge rate estimates and the MAGFLOW numerical code (Vicari et al. 2011, Ganci et al. 2012).

Paths of steepest descent has been used sSince 2007, by the Hawaiian Volcano Observatory (HVO) has used the paths of steepest descent to assess likely lava flow routes during effusive crises (Kauahikaua, 2007). DIn a recent example, during the 2018 eruption in the Puna district (Neal et al., 2019), the HVO produced preliminary lava flow path forecasts using the DOWNFLOW code (Favalli et al. 2005) . Later on, during the progression of the same effusive crisis, several lava flow paths from active flow fronts, new vents and overflow locations were simulated, so as to inform about probablelikely future lava flow directions. These maps were useful to assess the related hazard and provided situation awareness to stakeholders.

On Mount Etna, Italy, the Istituto Nazionale di Geofisica e Vulcanologia (INGV) at Etna Observatory (EO) is using an operational tool which combines satellite-derived discharge rate estimates and the MAGFLOW numerical code (Vicari et al. 2011, Ganci et al. 2012). The EO provides the simulation outputs to the Italian Civil Protection within the framework of an operational agreement aimed at minimizing the impact of lava flows.

At Piton de la Fournaise (La Reunion, France), the local Observatoire Volcanologique du Piton de la Fournaise (OVPF) is tacklingtackles the hazard related to the frequent effusive eruptions by combining the processing of satellite data with numerical lava flow modeling (Harris et al. 2017, 2019, Peltier et al., 2022). The OVPF has promoted an effective

collaboration between scientists affiliated to a multinational array of institutes and is able to ~~quickly~~ issue hazard maps based on DOWNFLOW (Favalli et al., 2005, Chevrel et al., 2021) and PyFLOWGO (Chevrel et al., 2018) within a few hours after the onset of an effusive eruption (Peltier et al., 2020).

In other recent effusive crisis such as the 2014-2015 Fogo eruption, Cape Verde lava flow hazards assessment was performed using both DOWNFLOW (Richter et al., 2016) and MAGFLOW (Capello et al., 2016b) codes, while the 2021 La Palma eruption used VORIS code (Felpeto et al., 2007; Carracedo et al., 2022;Marti et al., 2022).~~of an effusive eruption (Peltier et al., 2020).~~

Formatted: Not Highlight
Formatted: Not Highlight
Formatted: Not Highlight
Formatted: Not Highlight

1.2 Lava flow hazard modelling in Iceland

The first ~~L~~lava flow simulations during an eruption in Iceland was ~~first~~ done during the 2010 Fimmvörðuháls eruption with VORIS, which is an a~~utomatic~~ GIS-based ~~system~~ program for volcanic hazard assessment (Felpeto et al., 2007, Thorkelsson et al., 2012). The simulation was made to ~~describe a~~assess potential eruption scenarios ~~, with~~with ~~assumed~~ a given eruption location and runout length as input parameters. ~~This scenario was not updated as the eruption progressed.~~ Prior to the onset of the 2014-2015 Holuhraun eruption, VORIS ~~was~~ ran as part of the VOLCANBOX package (https://volcanbox.wordpress.com/) within the VeTools project (http://www.evevolcanoearlywarning.eu/vetools-objectives/) and ~~a~~ the early versions of a new Python-based stochastic model, MrLavaLoba started being run (de' Michieli Vitturi and Tarquini, 2018~~; Tarquini et al., 2019~~). During the unrest phase ~~prior~~ before the Holuhraun eruption, both VORIS and MrLavaLoba were run regularly and compared to each other. MrLavaLoba continued to be developed and improved throughout the eruption (Tarquini et al., 2019). After this eruption, both VORIS and MrLavaLoba were used for ~~Icelandic~~ volcanic hazard assessment projects in Iceland (~~https://skemman.is/handle/1946/24831, https://skemman.is/handle/1946/30779~~Andrésdóttir, 2016, 2018; Pfeffer et al., 2020). ~~https://www.vedur.is/media/vedurstofan-utgafa-2020/VI_2020_011_en.pdf).~~ Since 2015 the Icelandic Meteorological office, the Volcano Observatory in Iceland, has performed lava hazard assessments using the stochastic model MrLavaLoba. Both because of its fast computational time compared to more complex "deterministic" models that that have greater computational requirements, but also because its abilities to account for lava flow volume and the syn-eruptive modification of the topography compared to other stochastic codes.

Formatted: Pattern: Clear
Formatted: Not Highlight
Formatted: Not Highlight
Formatted: Not Highlight

2 Geological setting and eruptive history

Reykjanes Peninsula is an oblique spreading zone, characterized by eruptive fissures, open fissures and N-S striking strike-slip faults that are associated with the Mid-Atlantic plate boundary (e.g., Klein et al., 1977; Gee, 1998; Clifton and Kattenhorn, 2006; Einarsson et al., 2020, Sæmundsson et al., 2020). The eruptive centers have been divided into 4 – 6 volcanic systems (Fig. 1c), based on high-temperature geothermal areas, magnetic anomalies, eruptive centers, and geochemistry and are from East to West named: Hengill, Brennisteinfjöll, Krýsuvík, Fagradalsfjall, Svartsengi and Reykjanes (e.g., Jakobsson et al., 1978; Einarsson and Saeæmundsson, 1987; Einarsson et al., 2020, Sæmundsson et al., 2020).

The last four thousand years, vVolcanic activity on the Reykjanes Peninsula has been episodic, with several eruptions occurring in multiple volcanic systems over several hundred years followed by ~800–1000 years of quiescence. During the eruptive cycles of the last four thousand years this time Reykjanes, Svartsengi, Krýsuvík, Brennisteinsfjöll and Hengill volcanic systems were activehave erupted (Fig. 1c), while the Fagradalsfjall volcanic system remained inactive (Sæmundsson et al., 2020). The last most recent eruptive period of the Reykjanes Peninsula ended in 1240 CE (Sæmundsson et al., 2020). Basaltic subaerial volcanic activity has dominated the Reykjanes Peninsula since the termination of the last glaciation, estimated at around 12,000 – 15,000 years ago (e.g., Jakobsson et al., 1978; Saeæmundsson et al., 2010). The axial centers of the volcanic systems are dominated by eruption fissures, while shield volcanos lie on the periphery of each swarm (Jakobsson et al., 1978). The fissure eruptions were presumably short-lived, high effusion rate eruptions, while the shields are believed to be long-lived monogenetic eruptions that dominated the early postglacial times (Rossi, 1996, Jakobsson et al., 1978). During interglacial periods volcanic eruptions formed widespread glaciovolcanic edifices on the peninsula ranging from small mounds, tindars, flat-topped tuyas to multiple, polygenetic complexes of intergrown tindars and tuyas (Jones, 1969, Saemundsson Sæmundsson et al., 2010; Pedersen and Grosse, 2014). Mt. Fagradalsfjall and close surroundings islies in a complex of intergrown tuyas, tindars and mounds of different ages creating a complex topograpofhic diverse area with mountains ranging from 100-350 m elevation cut by nested enclosed valleys ranging from 50–215 m elevation. Around this glaciovolcanic complex there are postglacial lava fields gently dipping away from the complex in all directions (Sæmundsson et al., 2010).

2.1 Fagradalsfjall unrest and eruption

In the following section Fagradalsfjall 2021 unrest and eruption phases (Figure 2, column 1) are described with a focus on those characteristics of the eruption that affected the lava flow simulations performed at each stage (Figure 2, column 2).

Prior to the eruption, volcano-seismic unrest was detected at multiple volcanic systems (Svartsengi, Reykjanes and Krýsuvík) along the Reykjanes Peninsula. revealed by iIntense seismicity that started in December 2019 and ground

deformation revealing episodes of inflation and deflation ~~episodes~~ start~~inged~~ in January 2020 (Cubuk-Sabuncu et al. 2021, Floventz et al., 2022, ~~Geirsson et al., 2021~~Sigmundsson et al., 2022, Greenfield et al., 2022 Barsotti et al., ~~review~~2023). On February 24, 2021~~,~~ an intense earthquake swarm began with a ~~magnitude~~M_w 5.6~~4~~ located ~~2-3~~2-4 km NE of Fagradalsfjall marking ~~marked~~ the start of a dike intrusion. The location of the seismicity was both associated with the dike intrusion and the neighboring faults which were activated by induced stress changes in the crust (Sigmundsson et al, 2022). The dike continued to lengthen to approximately 9 km ~~and widen~~ during the next ~~3 weeks~~23 days before it erupt~~ur~~ed ~~East~~ east of Fagradalsfjall (Sigmundsson et al., 2022).

The eruption began on March 19 between 20:30 to 20:50 UTC in the Geldingadalir valley when a 180 m long fissure opened (Pedersen et al.,2022a, Barsotti et al., 2023). The fissure quickly concentrated into ~~a few vents, which after 2 weeks had concentrated on~~ two neighboring vents (Eibl et al., 2023). The lava started infilling the valley with a ~~fairly low~~ time-average discharge rate (TADR) ranging from 1 to ~~–~~8 m^3/s (Pedersen et al., ~~in press~~2022a). By April 5 a new phase of eruptive activity started as two new fissures opened 800 m northeast of the first fissure~~s. ,~~ ~~Anothe~~Further~~r~~ fissure opened at midnight on April 7, ~~one~~ on April 10 and ~~then two new fissures opened~~ on April 13. Each fissure concentrated into 1–2 circular vents, which over the following 10 days became inactive, except for the southern vent that developed from the April 13 fissures (Barsotti et al., 2023). By April 27 only one vent~~, which opened on April 13,~~ was ~~active~~active and remained active ~~, and remained the source of lava effusion~~ throughout the rest of the eruption (Barsotti et al., 2023). During thi~~s~~i~~s~~ vent migration phase the TADR ranged from 5 to 8 m^3/s (Pedersen et al., 2022a) and the lava started to flow into the valleys of Meradalir (April 5) and Syðri-Meradalur (April 14). From April 27 to June 28 the TADR increased from 9 m^3/s to a maximum of 13 m^3/s and with this increased effusion rate the lava migrated to its maximum extend~~t~~ 3.3 km from the active vent. The ~~through~~ lava was transported in systems of connected channels, lava ponds and tubes (Pedersen et al., in ~~press~~2022a). The lava "filled and spilled" to Nátthagi valley through Syðri-Meradalir (May 22) and through southern Geldingadalir (June 13). From June 28 to September 2 the lava effusion from the vent changed from being continuous to episodic ~~with intense lava emplacement~~ (ca. 12–24 hours of lava emplacement) followed by inactive periods of similar length (Barsotti et al., 2023). Despite this change, the ~~recorded~~ TADR in this phase ~~is~~was similar to the previous phase ranging from 9 to 11 m^3/s (Pedersen et al., 2022a). The episodic activity disrupted the dominant~~ing~~ lava transport system, causing large overflows in the vent region where an additional 50 m of lava piled up increasing ~~its~~ the total maximum lava thickness to 124 m (Pedersen et al., ~~in press~~2022a). In the last days of the eruption, ~~from~~ September 2 ~~to September -~~18, a 9-day-long pause (September 2–11) was followed by a week-long period (September 11-18) of activity ~~from September 11 to September 18~~(Pedersen et al., 2022a, Barsotti et al., 2023). Most of the lava ~~deposition~~ emplacement was in Geldingadalir, where a 10–15 m thick lava pond was established north-northwest of the active crater between September 11 to 15. The pond partly drained southward through an upwelling zone ~~southward~~ and into Nátthagi (September 15–18). The measured TADR was 12 m^3/s for September 9–17 and the final bulk volume of the lava flow-field increased to 150.8×10^6 m^3 covering an area of 4.85 km^2 (Pedersen et al., ~~in press~~2022a).

Formatted: Not Highlight

Formatted: Subscript

3 Data and Methods

3.1 Data

The primary data sources for lava flow simulations were the pre-eruptive and syn-eruptive digital elevation models (DEMs) that constitute the computational domain for the lava flow simulations.

IIn addition, in the pre-eruptive phase the lava flow simulations were initialized by using predefined, hypothetical, longer-term scenarios characterized by different fissure lengths and total volumes and fissure lengths. Two main volumetric eruptive scenarios were considered based on data from the eruptive history of Reykjanes Peninsula (The data, publicly available online, were extracted from the Catalogue of Icelandic Volcanoes which provides three main categories of eruptive scenarios for the volcanic systems considered for the unrest at Reykjanes peninsula (Sigurgeirsson and Einarsson, 2016; Einarsson, 2019a,b; Saemundsson, 2019; Sigurgeirsson and Einarsson, 2019; Óladóttir, 2022);. S comprisingpecifically, three total volumes were considered; a small and a medium-sized scenario characterized by volumes i.e. <0.1 km^3 (small scenario),and 0.1-0.5 km^3, respectively. Two lava flow fields: Illahraun (0.02 km^3) and Arnarseturhraun (0.3 km^3) served as a template for these scenarios (Sæmundsson et al., 2010) (medium) and >0.5 km^3 (large). The set of simulations were run accordingly with these three volumes. Two fissure lengths were chosen based on Jónsson (1978)´s geological data for the Reykjanes Peninsula; namely Previous eruptions on the peninsula are also known to have been featured through single vents, short fissures (2 km) and and/or long fissures (10 km). Given the uncertainty in the eruption setup during the unrest phase, a plethora of runs were undertaken to investigate the potential extension of lava flows for a combination of these parameters. Input data for the syn-eruptive phase Once the eruption started, therelied on available measurementsobservations of extruded volume and emitting vent geometry (Pedersen et al., 2022a, 2022b) and , were used for initializing simulations to produce the short-term and long-term hazard assessment.

3.1.1 Pre-eruption DEM

As pre-eruption DEM, Wwe used the 2 m-cell size IslandsDEMv0 (atlas.lmi.is/dem), as the pre-eruption DEM, a seamless mosaic of the ArcticDEM (Porter et al., 2018), with an improved positional accuracy and reduced amount of data outliers. Based on comparisons with lidar surveys carried out in the vicinity of the Icelandic glaciers (Jóhannesson et al., 2013), the elevation accuracy of the pre-eruption IslandsDEMv0 is better than 0.5 m (https://gatt.lmi.is/geonetwork/srv/eng/catalog.search#/metadata/e6712430-a63c-4ae5-9158-c89d16da6361). The cell size and number of cells of the computational domain (i.e., the DEM in grid format representing the local topography) has a strong impact on the performance of the MrLavaLoba code (Tarquini et al., 2019),-, as the number of grid cells increases, the simulation time increases For a given areal extent of the computational domain, a smaller cell size results in a higher the total number of grid cells, and thus in longer simulation time. Therefore, the IslandsDEMv0 was therefore down sampled to 5 m and 10 m cell size grids depending on the expected spatial extent of simulated scenarios. Large long-term scenarios (volume

> ~~50~~ 0.02 ~~M~~km^3) were simulated on 10 m cell size grids ~~10 × 10 m spatial resolution~~, while smaller short-term scenarios (volume < 0.02 km^3~~50 Mm^3~~) were simulated on 5 m cell size grids~~5 × 5 m spatial resolution~~. In a few ~~cases simulating~~simulations of lava flows close to barriers or within a narrow valley setting, the full resolution 2 m cell size ~~, 2 × 2 m,~~ of the IslandsDEMv0 was used as computational domain.

3.1.2 Syn-eruption photogrammetric surveys

Throughout the eruption, photogrammetric surveys were acquired as a part of the near real-time monitoring of the Fagradalsfjall 2021 eruption. These surveys consisted mainly of aerial photographs and Pléiades stereoimages and by September 30, 2021, 32 syn-eruptive surveys had been carried out. The acquisition and processing of these surveys are described in detail in Pedersen et al. (~~in press~~2022a) mainly following the semi-automated workflow of Belart et al. (2019) using the software MicMac (Pierrot Deseilligny et al., 2011, Rupnik et al., 2017), as well as Agisoft Metashape (version 1.7.3) and Pix4D mapper (version 4.6.4). Each of the surveys were co-registered to the pre-eruption DEM, i.e., the IslandsDEMv0, using the DEM co-registration method of the Nuth and Kääb (2011).

Each survey yielded DEMs (2 m cell size~~2 × 2 m~~) and orthomosaics (~~0.3 ×~~ 0.3 m cell size) from which the lava flow outline was obtained and this data is available via Pedersen et al. (2022b). By subtracting the DEMs with a pre-eruption DEM and with the DEMs from the previous surveys it was possible to obtain thickness maps (2 m cell size~~2 × 2 m~~) and estimate bulk eruption volumes and time-averaged discharge rates (TADR). These data products were generally available 3–6 hours after acquisition.

The thickness maps were used in the lava flow simulations for two purposes: (a) ~~aproved valuable for the lava flow simulation. Not only a~~s comparison to the ~~output of then~~results of lava flow simulations and (b) to update~~, but~~ the computational domain from pre-eruption to syn-eruptive topography ~~as the lava field became increasingly complex (after April 27), they were also implemented as a part of the computational domain~~ for the short-term simulation ~~updating the topography to the most current survey~~after April 27, when the lava field had become very complex to simulate.~~.~~

3.2 Methods

3.2.1 Software

MrLavaLoba is a probabilistic lava flow simulation code that was developed ~~by Mattia de' Michieli Vitturi and Simone Tarquini from INGV, Italy~~ starting in 2014 and first released ~~. The code was published~~ in 2018 (de' Michieli Vitturi and Tarquini, 2018)~~. and~~It is freely available at the model repository (http://demichie.github.io/MrLavaLoba/) ~~and it~~ and has previously been applied to the following eruptions: Etna 2001, Kilauea 2014–2016~~, and~~ Holuhraun 2014-15 and for hazard assessment of Heimaey (de' Michieli Vitturi and Tarquini, 2018; Tarquini et al., 2019, Pfeffer et al., 2020). ~~A~~ general introduction to the code is summarized below. For detailed technical explanation of the code we refer the reader to de'

Michieli Vitturi and Tarquini (2018) as well as the above mentioned ~~github~~GitHub repository ~~where code is commentated~~.~~Unpublished tests have also been carried out at Piton de la Fournaise (La Reunion, France) and on the 2014-2015 Fogo eruption (Cape Verde).~~

~~In~~ MrLavaLoba code requires (a) a computational domain constituted by the pre-emplacement topography and (b) a series of input parameters (including e.g., vent position and geometry, total extruded lava volume, the number of computational flows, and). ~~t~~The lava emplacement is simulated ~~is largely driven by the slope of the topography and by tunable input settings, while~~as elliptical lava „parcels“ or “lobes” with a given area and thickness that are deposited step-wise along the flow path ~~enabling continuous modification of~~constantly modifying the topography ~~as the lava is deposited~~. ~~In this way the code mimics that lava flows constantly create new topography within or on which new lava flows or lobes are deposited.~~ Each chain of a specified number of “parcels” making up a flow path is called a “flow”. The direction of propagation of the flow is determined by the direction of the steepest path descent (derived from the emplacement topography) and an “inertial” factor which considers the direction of the parent parcel with the addition of a random perturbation. Once the direction of propagation is determined, the new parcel is added in its final position. Another stochastic variable, the “lobe exponent”, controls the probability distribution among the existing parcels to bud to a new lobe (when this parameter is set to 0, the latest parcel emplaced generates the next lobe and no branching occurs). The code proceeds by iteratively setting new parcels on the topography until their total volume equals that prescribed volume for the simulation. For each simulation the code provides a raster of the final lava thickness and allows saving masked grids obtained by considering inundated cells fulfilling a specified threshold value. If this threshold is set to 95% (0.95), the thinnest portion of the final lava deposit representing 5% of the total volume is disregarded from the results. This step is important due to the probabilistic nature of the code, where the thinnest part of the inundated area represents a lower probability for inundation and may change between simulations despite having the same input parameters. The 95% masked grids from different simulations converge (de’ Michieli Vitturi and Tarquini, 2018) and represent an area “more likely” to be inundated. Through iterations of a large number of computational flows, MrLavaLoba handles the probabilistic aspect of lava emplacement (de’ Michieli Vitturi and Tarquini, 2018).

~~and the number of flows is an input parameter of the code. The code, given the lava volume, provides the final emplacement thickness of a lava flow field.~~

Additional topographical layers can easily be included in the model, such as lava thickness maps from syn-eruptive surveys or thickness maps of lava barriers allowing quick modification of the pre-emplacement topography (Fig. 3).

~~Beside a computational domain constituted by the pre-emplacement topography in grid format, the code requires to set a series of input parameters (including vent position, area of the parcels, cumulative volume, parameters that mimic style of emplacement, etc.). and an “inertial” factor with the addition of a random pertubation~~Several tuning options are implemented to mimic different lava transport mechanisms (channelized flow, lava tunnels or stochastic budding of lava

lobes) accounting for a given propensity to lengthening, widening or thickening of the flow field ~~(e.g., thickening parameter and thickening ratio)~~. ~~Additional topographical layers can also easily be included in the model, such as lava thickness maps from syn-eruptive surveys or lava barriers.~~

Examples of input settings written in a largely commented Python code can be found in the code repository (http://demichie.github.io/MrLavaLoba/). Furthermore, specific input parameters used in the pre-eruptive and syn-eruptive phase of the Fagradalsfjall 2021 unrest are provided in Table 1 (overview of the most important input parameters) and Table A1 (all input parameters).

Field Code Changed

~~Examples of input settings written in a largely commented Python code can be found in the code repository (http://demichie.github.io/MrLavaLoba/).~~

Field Code Changed

~~Additional topographical layers can also easily be included in the model, such as lava thickness maps from syn-eruptive surveys or lava barriers.~~ ~~When running the model, the lava is emplaced stepwise as elliptical parcels. The emplacement is the process of budding new parcels from the existing ones. The direction of propagation of the flow is determined by the direction of the steepest path (az_s) (derived from the emplacement topography) with the addition of a random perturbation (e_{az}) and an "inertial factor" which considers the direction of the parent parcel (az_p). Once the direction of propagation is determined, the new parcel is added in its final position. The area and thickness of each parcel is then added to the emplacement topography reflecting the deposition of lava, which constantly changes the pre-emplacement topography. Another stochastic variable, the "lobe exponent", controls the probability distribution among the existing parcels to bud a new lobe (when this parameter is set to 0, the latest parcel emplaced generates the next lobe and no branching occurs). The number of parcels in each flow, and the number of flows are input parameters in the code. The code proceeds by iteratively setting new parcels on the topography until their total volume equals that prescribed volume for the simulation. Several further tuning options are implemented to mimic different lava transport mechanisms (channelized flow, lava tunnels or stochastic budding of lava lobes) accounting for a given propensity to lengthening, widening or thickening of the flow field. In addition to the full inundated area, the code allows saving masked grids obtained by considering inundated cells fulfilling a specified threshold value. If this threshold is set to 0.95, the thinnest portion of the final lava deposit representing 5% of the total volume is disregarded from the results. This step is important due to the probabilistic nature of the code, where the thinnest part of the inundated area represents a lower probability for inundation and may change from one simulation to another given the same input parameters, while the masked area represents an area "more likely" to be inundated. Through iterations of a large number of flows, MrLavaLoba handles the probabilistic aspect of lava emplacement.~~

During the Fagradalsfjall eruption several new features have been implemented to improve ~~its~~ MrLavaLoba´s applicability to the ~~continuously changing conditions~~dynamic event (See section 4).. The ~~One of the~~ first change~~s~~ was to add the possibility to have multiple vents (or multiple fissures) active at the same time ~~and~~ with a prescribed supply probability. Second~~ly~~, the

code was modified to enable multiple threshold values for a single simulation, ~~in order to~~to filter inundated areas ~~according to~~ as differen~~t~~ting levels of ~~probability~~ likelihood of inundation ~~given a set of input parameters~~. Finally, the code was optimized to accelerate runs. With respect to the version available at the beginning of the Fagradalsfjall unrest, the optimized code now is up to 5-10 times faster. Appendix B provides details on the specific code changes and when they were implemented. ~~Finally, several code optimizations have been done to accelerate the code, both in the input/output procedures and in the computation of the flow emplacement. With respect to the version available at the beginning of the volcanic crisis, the code now is up to 7 times faster.~~

3.2.2 Implementation

A flow chart showing the implementation of input data and input parameters for the simulations, simulation results and evaluation can be found in Fig. 3. The implementation of MrLavaLoba code depended on the purpose of the simulation and ~~and~~ Ttable 1 provides a general overview of the simulation goals, approaches and ~~time-dependent/varying~~most important input parameters, while the full set of input parameters can be found in Ttable A1.

Since MrLavaLoba is a stochastic code, it ~~cannot provide the temporal evolution of the flow field for each run~~ does not describe the temporal evolution of the lava emplacement. However, by performing a series of runs simulating different volumes, it is possible to constrain the lava flow-field evolution by using the relationship V= Q * t, where V is volume, Q is the volume flux and t is the time. In the pre-eruption phase Q is a hypothetical effusion rate, while in the syn-eruption phase Q is derived from the TADR measurement performed at a given time. ~~this~~ We scaled the number of flows (n_flows) and lobes per flow (min_n_lobes and max_n_lobes) as a function of effusion rate and time. ~~However, since volume is one of the input parameters, the temporal aspect of lava flow-field evolution can be addressed by simulating various volumes and have input parameter such as number of flows (n_flows) and lobes per flow (min_n_ lobes & max_n_lobes) scalable based on the effusion rate and time~~. Thus, a higher effusion rate would provide more and longer flows from the vent ~~and longer flows~~ (so ~~higher~~larger n_flow ~~number~~ and ~~higher~~ min_n_lobe ~~number~~). ~~, and w~~With time the number of lobes would also increase (larger~~higher~~ min_n_lobe ~~number~~). In this way, insight to the temporal evolution of the lava field could be addressed. ~~either by pre-defined effusions rates, as used in the pre-eruption simulations, or based on measured TADR during syn-eruptive simulations. How these input parameters were scaled with effusion rate and time changed from the pre-eruptive to the syn-eruptive simulations. Both because there was more than one order of magnitude difference in effusion rate between the worst-case scenarios simulated in the pre-eruption simulations (300 m^3/s) and observed TADR during the eruption (mean TADR for the eruption was 9.5 m^3/s), but also because it was much harder to evaluate the results from the pre-eruptive scenarios compared to the syn-eruptive scenarios,~~

Formatted: Not Highlight

Formatted: Font: Not Bold

Formatted: Font: Not Bold

Formatted: Font: Not Bold

Formatted: Font: Not Bold

Formatted: Font: Not Bold

Formatted: Font: 10 pt, Not Bold

Formatted: Font: 10 pt, Not Bold

Formatted: Font: 10 pt, Not Bold

Formatted: Font: Not Bold

where lava flow simulations could be tuned to the observed lava flow thickness mapsThe exact tuning of n_flows and min-n-lobe can be found in Table 1 and Table A1..

4 Results

Different lava simulation strategies were implemented during the pre-eruptive unrest and during the eruption depending on the purpose of the simulation (Table 1). Overall, the purposes were three-fold:: (a) Prepre-eruption simulations to investigate the potentialrisk to infrastructure in immediate danger for lava flow inundation based on location of deformation signal, (b) syn-eruptive Ssimulations addressing areas ofto investigate short-term (two weeks) lava danger for lava flow inundationhazards (two weeks) and (c) syn-eruptive simulations to investigate addressing areas of danger for lava flow inundation in longlong-term (months to years) lava hazards.

4.1 Pre-eruption simulations

During the unrestThe pre-eruption lava flow simulations were initiated after seismic and crustal deformation InSAR data from February 23 to _March 1, 2021, revealed crustal deformation consistent with a 9 km long dike was detected intrusion causing intense seismicity (Geirsson et al., 2021Sigmundsson et al., 2022). The location of the seismicity was both associated with the dike intrusion, but also located on neighboring faults which were triggered by stress changes in the crust and not related to the intrusion of magma directly. Because of triggered seismicity along neighboring faults As a result, seismicity alone was n´ot specific enough to indicate where the dike that eventually erupted were migrating, and therefore a combination of seismic observations, deformation observations (cGPS and InSAR), stress modelling, and deformation modeling (Geirsson et al., 2021Sigmundsson et al., 2022) gave the best indication of potential fissure openings. Based on this information 12 different dike openings of 2-10 km length (See 3.1) were chosen for pre-eruptive lava flow simulations (Fig. 24a). These lengths were chosen with respect to length of visible eruptive fissures on the Reykjanes peninsula based on data from Jónsson (1978). It is considered very unlikely that an eruptive fissure of 10 km length will erupt on the western part of the Reykjanes peninsula but with respect to the worst-case scenarios a few lava flow simulations were run using this fissure length.

Two different strategies were implemented in this unrest phase:: (a) one short-term worst-case scenarios addressing areas likely to be inundated within a few hours from eruption start (relevant to emergency response planning) and (b) one for longer-term scenarios to providinge insight to insight to areas likely to be inundated within weeks to months (functionalrelevant for identification of infrastructure at risk) (Table 1, Fig. 2).

4.1.1 Short-term worst-case scenario

Formatted: Font: 10 pt, Not Bold
Formatted: Font: 10 pt, Not Bold
Formatted: Font: 10 pt, Not Bold
Formatted: Font: 10 pt, Not Bold
Formatted: Font: 10 pt, Not Bold
Formatted: Font: 10 pt, Not Bold
Formatted: Font: 10 pt, Not Bold
Formatted: Font: 10 pt, Not Bold
Formatted: Font: 10 pt, Not Bold
Formatted: Font: 10 pt, Not Bold
Formatted: Font: (Default) Times New Roman
Formatted: Line spacing: single

The worst-case scenario was defined as ~~a~~ fissure~~s~~ with an assumed effusion rate of 300 m^3/s, where~~, where t~~ the number of flows, n_flows = 300 and min_n_lobes were multiplied with 3.33 * per minute to mimic the lengthening of the flows (Table 1, Table A1). This multiplication factor was estimated to be rather high based on the run-out distance from the ~~vents after each time interval~~ vent but was preferred rather than being too conservative.

~~Using this approach, it was possible to evaluate areas of likely inundation hours after opening of a~~The results of the worst-case scenario~~s~~ for the 12 defined dike openings (see example Fig. ~~2b~~4b~~).~~

~~Based on the selected fissure openings and model set-up the results~~ suggested that no inhabited areas were in immediate danger ~~in~~during the first hours, and infrastructure was only in danger the first hours if the dike continued propagating south cross-cutting a nearby highway (Fig. ~~2a~~4a). ~~However, an~~A ~~obvious~~ caveat with this strategy was that the only way to validate the chosen parameter space was based on run-out distance and thickness of final deposit.

4.1.2 Long (er)-term scenario

~~Based on knowledge on lava volumes on the Reykjanes peninsula long term scenarios have been classified in three categories, small (<0.1 km^3), medium (0.1–0.5 km^3) and large (>0.5 km^3) (www.icelandicvolcanoes.is).~~ During the pre-eruption phase the small and medium eruption scenarios ~~were~~ simulated to evaluate potential endangered infrastructures. The tuning of these scenarios had been done before the volcanic unrest in Fagradalsfjall and is described in section 3.1 and input parameters can be found in Table 1 and A1.~~, since no large eruption scenario is known from the western part of the Reykjanes peninsula. Two different scenarios were run: small eruption scenario using the historical lava Illahraun (Volume= 0.02 km^3) as a reference, and moderate eruption scenario using the historical Arnarseturshraun (Volume= 0.3 km^3) as a reference. These scenarios were tuned to simulate lava length from 1–12 km with 5 km as the most likely result and lava thickness from 1–30 m with 10 m thickness as the most likely result.~~ An example of the moderate scenario is shown in Fig. ~~2b~~4c showing that the only infrastructure in danger were the nearby highway.~~.~~

4.2 Syn-eruptive simulations: short-term hazard assessments

During the eruption the complexity and demands of the short-term runs increased. Here we describe results from three different approaches applied during the crisis to address the evolution of eruptive activity and the challenges they posed (Fig. 2 and Table 1).~~:~~

~~I.First phase of the eruption: Geldingadalir (March 19–April 5)~~

~~II.Second phase: the vent migration phase (April 5–April 27)~~

~~III. Phase three to five: Fill and spill of a highly compound lava flow field (April 27–September 18)~~

Formatted: Space After: 0 pt, No bullets or numbering, Border: Top: (No border), Bottom: (No border), Left: (No border), Right: (No border), Between : (No border)

4.2.1 First phase of the eruption: Geldingadalir (March 19-April 5~~April 5-27~~)

~~After the eruption had started, we initiated t~~The first syn-eruptive runs of MrLavaLoba were started on March 19 around 22:00 UTC (1.5 hours after the eruption started) using preliminary vent coordinates ~~provided by the Civil Protection~~ obtained on a helicopter flight. ~~However, the precise~~The precise location and length of the fissure was first acquired the following morning when the first aerial images during daylight had been georeferenced ~~giving precise location and length of the fissure~~.

The main purpose of these first runs was to evaluate how the lava would ~~in~~fill the Geldingadalir valleys and when it would spill into Syðri-Meradalur ~~East~~ east of Geldingadalir, inundating the hiking path and ~~for hikers~~exposing ~~visiting the eruption~~visitors to lava hazards (Fig. 1, ~~3~~5, Table 1). ~~We remark here that MrLavaLoba does not provide a temporal evolution of the lava flow field, but by simulating different volumes and assuming a range of TADR, constrains on the timing of the spill into Syðri Meradalur and of the hiking paths inundation can be inferred.~~

During this phase we used a ~~stationary~~ 180 m fissure erupting ~~equally~~ with the same rate along ~~the fissure segment~~its extension, though in reality, ~~, despite the fact that~~ the ~~180 m long~~ fissure quickly concentrated into ~~a few vents and within 14 days, only~~ two active vents ~~were active in the northern end of the fissure.~~. This was done because ~~M~~mimicking the evolution of the fissure~~vent concentration from a fissure into a few points within a single simulation~~ either would have required a major change in the code, or ~~otherwise~~ a ~~would have required to develop a complex,~~ time-consuming, step-wise simulation strategy ~~that was impossible to fit in such~~inconvenient during "emergency-mode" ~~responding timeline~~response (Fig 2, column 2 & 3).

The lava simulations were qualitatively evaluated by comparing the thickness maps obtained from photogrammetric surveys with the modelled lava thickness maps ~~lava simulations~~. ~~However, f~~For the first hours of the eruption (<12 hr) the only documentation was from a few ~~very~~ oblique photographs. ~~Fig. 3 reveals that t~~The smallest run (V= 0.018Mm^3) shows northern and southern lobes agreeing with the photographs documenting the extent of the lava at midnight on March 19, ca. 3-4 hr after eruption start (Fig. 5). As the volume increased~~However, for the simulations with a volume between~~ to 0.2 – 3 Mm^3 ~~to 3Mm^3~~, the lava simulations overestimated ~~the extent of~~ the southern extent of the lava field, whilst underestimating the lava thickness of the northern lobe, which ~~can be~~is explained ~~with~~ by the closing of the ~~vents to the South~~southern part of the fissure. As the volume increased further~~However, for the simulations with volume between~~ to 3-7 Mm^3 the modelled results agreed ~~fairly~~ well with the observations suggesting that the lava ~~at this point~~ was so confined by the Geldingadalir valley that the change in vent geometry had little effect on the lava inundation area.

The simulations predicted ~~that~~ at potential exit from Geldingadalir valley into Syðri-Meradalir valley when the volume reached ~~from~~ 7 – 10 Mm^3, with slightly different volumes from run to run due to the stochastic nature of the MrLavaLoba

code. ~~The TADR estimates obtained from photogrammetry in this phase ranged from 1–8 m³/s with a mean of 4.9 ± 0.1 m³/s.~~ ~~In order~~ To ~~to~~ provide potential timings of when Geldingadalir would ~~fill and~~ spill into the Syðri-Meradalir valley we used two different effusion rates of ~~a maximum effusion rate of 10~~8 m^3/s and 5 m^3/s based on the observed maximum and mean TADR estimates in this phase (Pedersen et al., 2022a) ~~to provide a minimum time for when the valley potentially would spill~~. This gave ~~a minimum time of~~exit times from Geldingadalir of ~~8~~ 12 days after eruption start (so March 27 ~~-31) before exit from Geldingadalir. For 8 m³/s it would be~~ 10-14 days (March 29 -April 2) and ~~and for the 5 m³/s it would be 11~~6-24 days (April 4-April 12), respectively. The lava eventually spilled out from Geldingadalir valley on April 14, but by April 5 new vents had opened ~~North~~ north of Geldingadalir, with lava draining ~~the lava supply from the initial vent~~into Meradalir. ~~The measured total TADR for all vents between April 5–18 was between 5–8 m³/s, however the majority of the lava at this point were deposited in Meradalir and the plateau NE of the Geldingadalir vent.~~ By calculating the lava volume within Geldingadalir by April 18 (first photogrammetric survey after lava exited Geldingadalir) we get a volume of 10.8 Mm^3, ~~whilst the total erupted volume was 16.1 Mm³ (first photogrammetric survey after lava exited Geldingadalir 4 days earlier).~~ The 10.8 Mm^3 is in the upper end of the predicted volume of 7 – 10 Mm^3, ~~for lava exiting Geldingadalir of the simulations,~~ but taking into account 10.8 Mm^3 is the volume in Geldingadalir four days after the lava spilled into Syðri-Meradalir, we find this in good agreement with the lava simulations. ~~still within reasonable agreement.~~

4.2.2 Second phase: Vent migration (April 5-April 27) ~~Second phase: Vent migration~~

In the second phase ~~2 (April 5 to April 27)~~ the active vents migrated as~~d~~ multiple new fissures opened between April 5-13 and became inactive over the next 10 days, except for one vent (see section 2.1, Fig. 1). ~~Multiple eruption fissures opened, starting on April 5, when two new fissures opened 800 m northeast of the first fissure. Another fissure opened at midnight on April 7, another one on April 10 and then on April 13 two new fissures opened. Each fissure concentrated into 1–2 circular vents which, over the following 10 days, became inactive, except for the southern vents that developed from the April 13 fissures. All of these fissures had variable effusion rates.~~

This change in eruption activity provided new challenges to the lava flow modelling ~~, which are illustrated in (~~Fig. 4~~2~~). The first challenge was that the topography drastically changed with the new vent openings. ~~From~~ While lavas ~~being~~were strongly constrained within the Geldingadalir valley in the first phase, ~~the lava was~~ after April 5 lava was issued from the plateau NE of Geldingadalir and channelized into narrow gullies before spreading out like a fan within the Meradalir valley ~~(Fig 4)~~. ~~The new vents~~Fissure 2, that opened April 5, had sufficient spacing ~~that from~~the activity in Geldingadalir ~~and at fissure 2~~so it could be simulated in a separate run from Geldingadalir~~two different runs~~ (Fig.~~4~~6, V< 0.4 Mm^3). However, to capture the channelizing into the narrow valleys it was necessary to increase the resolution of the computational domain DEM (from 5 to 2 m cell size~~5 m to 2 m cellsize~~) and change the lobe exponent parameter (from 0.07 to 0.03) ~~(thus~~

increasing the probability of new lobes to be generated by younger lobes~~)~~ (Fig. 2). ~~Lower DEM resolution and higher lobe exponent caused over spilling from one valley to another earlier than observed in the eruption~~After this adjustment the new flows were well captured in the simulation (Fig.6, V< 0.4 Mm^3).

~~The second challenge was that a~~After fissure 3 opened on April 7, it was clear that the lava flows from the ~~active~~ different vents were influencing ~~each other~~each other, and it was therefore necessary to simulate multiple vents that emitted variable percentages of the total lava volume. The MrLavaLoba code was ~~then~~ therefore modified to allow this ~~configuration~~configuration (See section 3.2.1, Fig. 2 and Appendix B)~~, and from this stage and onwards it was possible to simulate multiple vents simultaneously~~ . ~~However, there was very little available information~~ available on the variable percentages of the total lava volume ~~each vent emitted.~~ Qualitative estimates on the variable percentages from each vent~~were made~~ were based on webcams and direct observations in the field with no direct way of validating these estimates.

~~–~~As the lava flow field emplacement progressed, it became evident that it was necessary to include the most recent lava thickness maps from the photogrammetric surveys (Pedersen et al., 2022a). By adding ~~Thereby~~the thickness maps on top of the pre-eruption DEM~~the computational domain was updated~~, and new simulations ~~could be~~were performed on the most updated topography. Examples of two runs with two different vent configurations can be found in figure 6, lowermost panel: one with all vents being active (left) and one performed after the two northernmost vents had shut down (right). These simulations ~~did~~ showed how the lava would expand in Geldingadalir and ~~into~~ the neighboring valleys: Syðri-Meradalur and Meradalir. However, the expansion in Geldingadalir and the plateau NE were overestimated and the expansion into Meradalir was underestimated. We ascribed this ~~However, by doing so another problem arose~~to a problem~~; namely what~~ that we ~~called~~refer to as the “restart problem” (Fig. 2). By restarting the simulation ~~After including updated topography, the code would start simulating a new eruption~~on updated topography, ~~where~~ the lava parcels would be initiated from the vent~~s~~s resulting in increased lava deposition close to the vents (explaining the overestimation of Geldingadalir and the plateau NE) and a delay in expansion of the lava field far away from the vents (such as Meradalir) compared to the real flow-field~~,~~ ~~meaning that it would require a given number of parcels before the edges of the lava field would be activated again creating a delay in the areal expansion of the simulated lava field compared to the real flow-field~~.

~~Figure 4 show two runs with two different vent configurations; one with all vents being active and one performed after the two northernmost vents had shut down (Fig. 4, lowermost panel). These simulations did show how the lava would expand into the neighboring valleys: Syðri-Meradalur and Meradalir. However due to restart problem, some of the results underestimated the expansion of the lava field into Meradalir, whilst other areas (e.g., Geldingadalir and the plateau NE of Geldingadalir) were overestimated, probably due to incorrect ratios of emitted volume between active vents.~~

4.2.3 Phases three to five: Fill and spill of a highly compound lava flow field (April 27-September 18)~~Third to fifth phase: Fill and spill of highly compound lava flow field~~

After April 27 the vent activity stabilized ~~to~~at one location (Fig. 1, Vent 5). The mean TADR increased from 6 m^3/s to 11 m^3/s (Pedersen et al., 2022a). The lava flow-field expanded into neighboring valleys such as Nátthagi and further into Meradalir in a "fill and spill" process. There was great interest in simulations that forecasted when and how the lava might overflow from one valley to another e.g., from Geldingadalir into Nátthagi (cross cutting a popular hiking path) or when the lava would exit from the Meradalir valley (inundating a dirt road), or when it would exit Nátthagi (threatening a highway and critical communication cables, as well as approaching the sea). However, due to the restart problem (see 4.2.2) and because the lava discharge into different valleys was highly variable ~~switching from one valley to another in an unpredictable manner~~ (Pedersen et al., 2022a~~in press~~), it was ~~therefore~~ decided to address these questions related to ~~the~~ short-term hazard~~s of lava exiting from a valley with~~using worst-case scenario approache~~s~~. These scenarios were presented at bi-weekly stakeholder meetings, where the aim was to ~~(i)~~ identify hazardous areas (upcoming inundation of hiking paths, roads or installed infrastructure) and suggest potential closure of areas to public access (e.g., closing of Nátthagakriki in September 2021); . ~~(ii) create awareness of potential upcoming inundation of hiking paths, roads and installed infrastructure, and (iii) suggest where to close areas closed for public access (e.g., closing of Nátthagikríka in September 2021).~~

In these simulat~~ed scenarios~~ions, the most recent TADR estimate (Pedersen et al., 2022a) ~~based on the most recent photogrammetric survey~~ was used to calculate lava volumes that would be ~~equal to set time~~extruded over periods of 3, 7, and 14 days. These volumes were then released at critical lava ~~front~~ margins close to valley exits ~~in order to~~to evaluate if each given volume was sufficient to overflow the valley in the given timeframe. If a 3-day scenario would spill out of the valley, then 6 hr, 12 hr and 24 hr scenarios ~~would be~~were additionally modelled ~~as well~~. The critical locations were selected ~~by the modeler qualitatively~~ considering the location~~based on knowledge o~~ of hiking paths and infrastructures.
In these runs, the input parameter for the "number of flows" (n_flows) was doubled (from 80 to 160, Table 1), both because of the increase of the TADR, and to~~because we found that having more than 100 flows results in a~~ reduce~~d~~ the uncertainty in the simulation outputs (Fig. 7 in de~~"~~" Michieli Vitturi and Tarquini, 2018).

An example of how these worst-case scenarios were presented at ~~the~~stakeholder meetings ~~with the stakeholders~~ is provided in ~~f~~Fig. ~~5~~7. To simplify the maps, ~~we only decided only to show~~ the lava inundation area and not the simulated lava thickness maps was presented in accordance with the stakeholders interest~~and not the simulated lava thickness maps~~. ~~In this way,~~T ~~t~~he results for the volumes extruded ~~t~~over 3, 7 and 14 days ~~could be~~were displayed in one map. The main map (Fig.~~5a~~7a), show~~s~~ simulations from vent 5 and was considered the most likely scenario, while the four smaller ~~panels~~ maps show the same volume~~ss~~ released at ~~the~~ defined critical locations (Fig.~~5b~~7b-e). As it can be seen by the provided example from September 9, 2021, both the Meradalir, Geldingadalir and Nátthagi valleys ~~could~~ had the potential to overflow, ~~given~~ if the lava was

transported to the critical ~~points that were used as simulated vents~~lava margins.~~ The main~~A weakness of this approach ~~is~~ was that the location of critical lava margins ~~hypothetical outbreaks areas arbitrarily~~ were manually selected on the basis of the available knowledge and expert evaluation ~~and are subject to a large uncertainty~~. ~~Furthermore, re-tuning of the code to simulate lava poured from lava front edges rather than the actual vent is a more difficult task, since most of these hypothetical outbreaks did not happen.~~

A similar approach was used to test lava barriers that were buil~~t~~d or planned to be built during the eruption. An example can be found in ~~f~~Fig. ~~6~~8, where the overflow of Geldingadalir was simulated with and without barriers based on photogrammetric data from a survey on June 11, 2021. All scenarios show that with 1 Mm^3 volume of lava Geldingadalir w~~ill~~ould overflow into Nátthagi. ~~For no~~In absence of barriers ~~it will~~ lava would also spill west into Nátthag~~i~~a kr~~í~~i~~k~~i~~a, but with the proposed barriers it seemed plausible to stall the west-ward migration~~, at least~~ for small volumes. Once again, these were worst-case scenarios, because (~~i~~a) they required that the given volume of lava ~~is~~ was transported to the ~~simulated vent~~critical margin, and (~~ii~~b) the simulations assume~~dd~~ that the transport systems near the barrier ~~is was not efficient and promotes~~ promoted the lava piling up near the barrier. However, if an efficient ~~lava transport system develops~~channel or tube developed, the majority of the lava would be transported into the Nátthagi valley resulting in ~~a~~little lava deposition ~~little amount of lava would pile up close to~~at the barriers, meaning that ~~they~~the barrier would last longer.

Formatted: Not Highlight

4.3 Long-term runs

Stakeholders (managers of critical infrastructure, municipalities, civil protection authorities) requested long-term scenarios for longer-term planning and we were aiming to provide them in September 2021. The eruption stopped September 18, ~~The long-term scenarios were planned to be released to end-users (managers of critical infrastructure, municipalities, civil protection authorities) in September 2021 and were requested from stakeholders for longer term planning. However, the eruption came to a halt on September 18, and these scenarios were not officially released bu~~and these results were therefore only ~~t just~~ presented at stakeholder meetings ~~with stakeholders~~. The ~~Long~~long-term scenarios were simulated by considering erupted lava volumes ranging ~~from~~ between 250 Mm^3 ~~to~~ – 5000 Mm^3. Assuming constant ~~If the~~ mean TADR of 9.5 m^3/s (Pedersen et al., 2022a) ~~is~~were ~~assumed to be always equal to the mean TADR for~~across the entire eruption ~~(9.5 m^3/s, Pedersen et al., 2022a~~in press), ~~it turns out that these~~the simulated long-term scenarios would cover time frames of half a year to decades.

In these large simulations only one vent (vent 5 in Fig. 1) was active throughout the simulation, which had been the case for most of the eruption. Furthermore, each scenario was obtained as a single run (with a single tuning) and not as an iterative process of tuning the model step by step. We tuned the long-term runs against the lava thickness maps obtained in June 2021

having volumes between 53-80 Mm^3 and preferred to overestimate rather than underestimate lava inundation area. Fig. 9 shows that the full extent of the long-term model for 80 Mm^3 (top row, center) fits the real lava deposit very well in both extent and thickness (bottom row, center), except around the NE plateau which is explained by the model only having vent 5 as the active vent. The thickening close to the vent was underestimated and the thickening in Meradalir was overestimated.

~~(vent 5 in Fig. 1)To simplify these large simulations only one vent was considered active (vent no. 5 in Fig. 1) throughout for~~ the entire ~~the simulation, which had been the case since April 27, 2021. Furthermore, each scenario was obtained as a single run (with a single tuning) and not as a series of runs with an iterative process of tuning the model step by step. We tuned the long-term runs against the lava thickness maps obtained in June having volumes between 53-80 Mm^3 and preferred to overestimate rather than underestimate lava deposits~~inundation area. ~~Fig. 7 shows the thickness maps obtained by the airborne photogrammetry and the simulation results for 80 Mm^3. As can be seen this model set-up does not include lava on the northeast plateau north of vent 5, which is due to the fact that as the long-term simulation is based on a single active vent (Fig. .7, top row) and therefore neglects the actual lava extrusion which occurred multiple vents Before April 27, 2021. Generally, the fit is acceptable, although the thickening close to the vent was underestimated and the thickening in the Meradalir valley was overestimated.~~

The long-term hazard assessment was specifically intended for stakeholders with no experience with lava flow simulation and like the short-term worst-case scenario maps produced in phase 3-5 (See section 4.2.3, Table 1) we choose only to display the lava inundation area, since this was the main interest to stakeholders. ~~These long-term models were specifically intended for stakeholders with no experience with lava flow simulation.~~ The new challenge was ~~therefore~~ how to communicate the uncertainty in our results to non-experts (Pallister et al., 2019). We decided to create maps where lava inundation would be divided into three qualitative categories: "~~very~~ more likely", "likely" and "less likely" (Fig. ~~7~~9, left bottom row). We defined the "more likely" category to be the 95% masked grid (See 3.2.1), which filter out the places least likely to be inundated (Fig. 9 top left). The full extent of the lava simulation was decided to be categorized as "likely" (Fig. 9 top center). For the "less-likely" category~~Thus, like the worst-case scenario maps produced in phase 3-5 we would not display the thickness maps, but simply the lava inundation area, since this is~~was the ~~of main interest to stakeholders.~~

~~The code of MrLavaLoba is not designed to communicate uncertainty of the results, and it was therefore necessary to come up with a strategy to define these categories. The full extent of the lava simulation was decided to be categorised as "likely". This result would be based on the input parameters derived from the tuning, but the extent of the thinnest lava deposits would vary from simulation to simulation due to the stochastic behavior of the code. De' Michieli Vitturi and Tarquini, (2018) noted that by using a 95% mask showing the thickest 95% of the deposit (i.e., disregarding the 5% of volume given by the thinnest part of the deposit) the results from different simulation would converge to a given coverage. Thus, by using~~

~~the 95% mask the results are filtered removing the places least likely to be inundate and it was therefore decided to use the 95 % mask as the "very likely" category.~~

~~However,~~ we ~~also~~ wanted to communicate the uncertainty related to the model tuning. ~~Especially because the~~We tuned the model when the lava flow field was highly constrained by the surrounding topography. However, in a large eruption the lava would escape the confining valleys and be able to spread more freely over flat-lying areas. ~~tuning parameters were derived when the lava flow field were highly constrained by the surrounding topography (Fagradalsfjalls mountains and valleys) whilst the large scenarios would inundate the low sloping areas outside the Fagradalsfjalls area, where the lava flow field could spread more freely over flat lying areas. However, at this point we did not have a quantitative approach for addressing this issue, and instead,~~ To display this uncertainty, it was decided to change the tuning of the "lobe exponent" (from 0.02 to 0.01) which is crucial parameter for the lava flow spreading. A lower lobe exponent ~~would~~ promotes lower flow thickness and a longer run out length as revealed in our tuning data set overestimating the inundation area~~.~~ (Fig. 9 top right). ~~Choosing a lower lobe exponent (0.01 instead of 0.02) that largely overestimate the inundated area of our tuning data set (Lava thickness maps from June) wer~~We therefore defined this~~e therefore used as a route to communicate scenarios that, based on our tuning data set,~~ as the ~~were~~ "less likely" category. ~~, but could not be excluded due to the very changeable topography in the area (Fig.7, top row).~~

One example of the ~~produced~~ long-term hazard maps can be found in Fig. ~~8~~10. ~~The main take home~~most important message for the authorities from these long-term simulations ~~is~~ was that none of the runs reached Grindavík town nor the Svartsengi powerplant, which ~~are~~were the two ~~of the~~ main ~~inhabited and infrastructure~~ areas of ~~closest to the eruption site~~concern. ~~However,~~We ~~it is important to~~ underlined that these long-term runs ~~are~~ were quite uncertain, because as the scenario grows in volume so does the uncertainty. Some factors contributing to uncertainty were: (a) ~~In addition to the~~ tuning being undertaken while the lava was highly controlled by topography, (b) changes in eruptive activity from~~, the following additional challenge was encountered. The style of eruptive activity varied between~~ continuous (May-June, when tuning were performed) ~~to fountaining~~ to episodic activity (July-September) ~~(12-24 hours of quiescence). These changes impacted the efficiency~~and (c) ~~of the lava transport mechanisms~~ emplacement ~~(Pedersen et al., in press). When the tuning was performed, the activity was fountaining and had transport systems that enabled lava emplacement from the edges of the lava flow field about 3.3 km from the vent. In July, instead, the activity was episodic, and resulted in a shortened lava transport systems with lava preferentially stacked close to the vents. Another point of concern is~~ that the current version of MrLavaLoba does not include vent processes such as cone build-up. The latter was ~~This was~~ important because the real vent built up faster than predicted in the simulation, meaning that the lava flows might had inundated Fagradalsfjall faster than predicted in these models.

5 Discussion

5.1 MrLavaLoba code: ~~Pros and cons~~Advantages and disadvantages

~~How the MrLavaLoba code was implemented and developed during the pre-eruptive and syn-eruptive stage of the Fagradalsfjall 2021 crisis has been described in the results. The flexibility of t~~The MrLavaLoba code ~~made it possible to implement use it in different way for different purposes, which is unique amongst the existing stochastic codes. The MrLavaLoba code~~ is freely available, easy to run, ~~coded in Python, in Python, and~~ computationally fast and ~~(especially after the optimizations carried on during this work). It~~ can ~~thus~~therefore be used to tackle large volume scenarios (Table 2). Unlike other stochastic codes it ~~includes~~ accounts for lava volume ~~and~~and estimates final lava extent, it produces lava thickness ~~layers~~layers, and it models ongoing topographic changes during the simulation. Th~~i~~eses characteristics w~~as~~ere very important during the Fagradalsfjall 2021 eruption~~crisis~~, because assessing the timing of ~~the~~ hazards related to the fill and spill of nested valley systems only could ~~not have been~~be addressed by codes that ~~do not include~~ accounted for lava volume. It was easy to implement topographic changes into the model, including the syn-eruptive differential DEMs of the lava flow thickness and lava barriers, which was key for testing both ~~suggested~~ hypothetical barriers and built lava barriers (Table 2). However, there were also weaknesses to the code~~drawbacks relying on the MrLavaLoba code;: including the fact that it~~ MrLavaLoba ~~is a stochastic code and not a physical code, such that it~~ does not provide temporal evolution of the lava field during each run, nor does it directly provide velocity estimates of the lava emplacement (Table 2). Input parameters must be tuned for specific eruptive scenarios and locations~~. The tuning will be different for different volcanic systems, different topographic conditions and different sizes of scenarios~~. It is possible to mimic different lava emplacement processes (e.g., lava channels or tubes), but this ~~has to~~must be tuned as well ~~and ideally all of this tuning has to be completed before a volcanic unrest~~. Furthermore, ~~it became a concern for the long-term scenarios, that~~ the code does not include vent-processes, which lead to an underestimation of the lava thickness close to the vent for the long-term scenarios. ~~This limitation impacted the capability of forecasting for when Geldingadalir valley would be filled and thus when lava could migrate westward over the Fagradalsfjall plateau towards critical infrastructure.~~ However, to our knowledge, no existing lava simulation code includes vent-processes, so this issue would also have a~~ffectppli~~ed ~~to all~~any other lava flow simulation codes. ~~Probably, this is mainly an issue for eruptions in flat terrain or within nested valleys, and not on steep slopes that will dictate the flow direction and deposition independent of localized changes at the vent.~~

~~The following discussion will focus on the lessons learned so far; the improvements of the code, the implemented modelling approaches and the dissemination of results for hazard communication purposes. We will discuss the current caveats and how the code, approaches and dissemination strategies could be improved for the next volcanic crisis.~~

Formatted: Font: 10 pt, Bold

Formatted: Font: 10 pt, Bold

Formatted: Font: Bold

5.~~1~~ 2 Towards improved modelling ~~MrLavaLoba code~~

To improve our communication of uncertainty of the lava simulations MrLavaLoba was upgraded in September 2021 to enable multiple masked lava thickness grids (section 3.2.1, appendix B). In the future we can therefore provide maps with uncertainty comprised of the full extent (100 % mask) of the lava flow simulation, the 95% mask and e.g., the 68% mask indicating the likelihood of inundation. In addition, we would like to evaluate of the uncertainty of the input parameters themselves, which can be addressed by using statistical tools such as Dakota (Adams et al., 2021), which specifically designed to perform sensitivity analysis and uncertainty quantification with existing numerical codes (Fig, 3 see bottom row).

In the Fagradalsfjall 2021 eruption the lava flow simulations were evaluated qualitatively (Table 1, Fig. 3), but a quantitative approach would have been preferred. For future eruptions we would like to automate a quantitative comparison between two rasters (e.g., simulation and observation) with respect to the accuracy of the estimated (a) lava inundation area and (b) lava thickness. This can be done by using the Python script *union_diff.py* available in the model repository (http://demichie.github.io/MrLavaLoba/), which permits such comparisons (Fig. 3 see bottom row).

~~Three main issues with the code were identified and addressed during the Fagradalsfjall 2021 eruption, namely (a) implementation of multiple vents, (b) implementation of multiple masks and (c) scaling issues with changes of resolution of the computational domain. Here we describe how these issues were addressed.~~

Commented [GBMPH1]: Think of fig2

Vent changes (temporal change in vent configuration and geometry, vent build-up and collapse) remained a challenge for the lava simulations during the eruption. This problem was partly solved in April 2021 when the MrLavaLoba code was upgraded ~~During the vent migration phase (Phase 2) multiple vents were active at the same time, and it was therefore needed~~ to simulate multiple vents ~~in the same run, allowing lava emplacement from multiple source locations to influence each other. The model capability has been described in~~(See section 3.2.1, appendix B~~xx~~) and thus ~~and was used from the beginning of April and onwards~~. ~~This model option requires, in addition to the coordinates of all active vents, their relative supply probability, which is a ratio defining how the supply rate is divided among the active vents. Two issues were found with this implementation. First of all, retrieving information on supply probability was difficult based on observation and thus the modeller was forced to make very rough~~ and subjective ~~estimates of this ratio. This challenge reflects the interplay between the limitations of lava flow monitoring and the issues for the person modelling. Secondly, in the eruption, different vents turned on and off at different times, but this temporal source variation is unlikely able to be implemented in MrLavaLoba because there is no „time“ in the simulations. In practice,~~ the modeler ~~began~~ initialized a new lava simulation when the number of active vents changed. ~~Finally,~~ Doing step-wise simulations was possible since we could do simulations on updated topography~~updating the computational domain through incorporation of ancillary data such as syn-eruptive~~

~~DEMs or lava thickness maps~~. This strategy ~~in lava simulations have~~s been ~~thought of~~intended as a route to improve lava flow simulations ~~bypassing caveats of lava simulation codes to~~and ~~reproduce~~ing the lava flow-fields more consistently (Harris et al., 2016, Tarquini et al., 2018). However, as we discovered, updating the topographic domain created a new problem~~:~~; namely the restart problem (~~described in~~See 4.2.2)~~:, where the real eruption was continuously transporting lava to the edges of the flow-field while t~~the re-initialized simulation experienced a delay in the lava field expansion~~, as the simulation required a „spin up time" to get lava advancing at the edges. We have learned that discretizing lava simulations into sequential separate simulations with updated topography will require a strategy to deal with this "spin up time". ~~This problem is not unique to MrLavaLoba, but relevant for all lava flow simulation code that intend to do step-wise simulations. This issue is not specific to the MrLavaLoba code but will likely apply to all lava simulation codes that attempt to sequentially introduce new starting conditions to implement time evolution.~~Some potential ways forward to

~~We propose some potential ways forward to~~ solve this could include~~:~~ introducing

~~1) integrate lava transport system~~

~~2) Find a way of having a~~ „spin up"~~-~~time that will re-establish activity ~~at~~to the flow field edges~~.~~, or

~~3) I~~implement additional sources at active lava margins as we did for the worst-case scenario runs (~~described in~~See 4.2.3).

Finally, a remaining challenge is related to changing the spatial resolution of computational domain in the simulations. Some input parameters need to be re-tuned if the input DEM resolution is changed. Tuning takes time, which is inconvenient during an on-going eruption. As a rule of thumb, the lobe area is 10 x (DEM cell size)^2. If the lobe area changes by a factor G, the number of lobes should change by a factor 1/sqrt(G) for scenarios with a lobe exponent= 0. For other scenarios experimentation with the code and different DEM resolutions could provide us with an automatically applied scaling of these sensitive parameters in case of DEM resolution changes.

~~In the beginning of September, issues about communicating uncertainty came to the forefront. The model was upgraded to save multiple mask output levels, which has been described in section 3.2.1. This feature was primarily used after the eruption ended to show the full extent (100 % mask) of the lava flow simulation, the 95% mask and e.g., the 68% mask on a map indicating the likelihood of inundation. The lowest mask threshold indicates the thickest lava deposits and thus the areas, that are most likely to be inundated, and the three masks were therefore used to communicate the uncertainty related to the fact that MrLavaLoba is a probabilistic model and is specific to a given set of input parameters. In the future the quality of these mask thresholds should be tested routinely by repeating each simulation scenario to ensure that the masked results of repeated runs are consistent. Such a consistency indicates that the number of flows in a scenario is adequate for the given thresholds to indicate likelihood (de' Michieli Vitturi and Tarquini 2018).~~

Formatted: Space Before: 0 pt, After: 0 pt

Formatted: Line spacing: 1.5 lines

Formatted: Superscript

Some of the input parameters are sensitive to the spatial resolution of the computational domain and thus need to be re-tuned if the input DEM resolution is changed (for example if using a coarser DEM over a larger domain for long-term scenarios). It is time-consuming to tune the input parameters, and this can be impractical while a volcanic crisis is ongoing.

In the specific case of no branching (lobe_exponent=0), we observe that the maximum runout of a simulated lava flow is proportional to the major axis of the ellipical parcels and the number of lobes in each lobe chain. Thus, when the DEM resolution is changed, and the lobe area is scaled proportionally to optimize the computational cost, the number of lobes in each chain also must be changed in order to attain a similar runout. In this case, if the lobe area changes by a factor G, the number of lobes should change by a factor 1/sqrt(G). When lobe_exponent>0, the definition of the scaling factor is less obvious. In fact, the larger the number of lobes, the larger is the occurrence of branchings, and a tuning is needed to reproduce the same runout.

5.2 Modelling approach: pros and cons

Formatted: Normal, Line spacing: 1.5 lines

Both in the pre-eruptive and syn-eruptive phases of the Fagradalsfjall 2021 volcanic crisis the modelling approaches were divided into two categories; 1) a short-term scenarios addressing hazards on a time scale of hours to days and 2) long-term scenarios focusing on hazards relevant on timescales from months to years.

Formatted: Normal, Line spacing: single, Font Alignment: Auto

These scenarios were evaluated qualitatively (table 1), but ideally a quantitative approach should have been implemented beforehand. Thus, for the scenarios where it was possible to compare simulated lava thickness maps with lava thickness obtained by photogrammetry it would have been viable to quantitatively compare the two rasters with respect to the accuracy of (a) estimated lava inundation area and (b) lava thickness.

For future eruptions it will be possible to use the Python script *union_diff.py* available in the model repository (http://demichie.github.io/MrLavaLoba/). It compares raster files defined on the same grid, meaning that they have the same spatial resolution and spatial extent and produces different outputs.

First, it computes the Jaccard similarity index, defined as the area of the intersection of two deposits divided by the size of their union. This index, as discussed in de' Michieli Vitturi and Tarquini (2018), can be used to assess the convergence of the masked outputs when the number of flows is increased. The script also computes the average thickness difference between two rasters, and thus it can be used not only to compare two outputs of the model, but also simulated thickness maps with observed lava thickness.

In the beginning of September, issues about communicating uncertainty came to the forefront. The model was upgraded to save multiple mask output levels, which has been described in section 3.2.1. This feature was primarily used after the eruption ended to show the full extent (100 % mask) of the lava flow simulation, the 95% mask and e.g., the 68% mask on a map indicating the likelihood of inundation. The lowest mask threshold indicates the thickest lava deposits and thus the areas, that are most likely to be inundated, and the three masks were therefore used to communicate the uncertainty related to the fact that MrLavaLoba is a probabilistic model and is specific to a given set of input parameters. In the future the quality of these mask thresholds should be tested routinely by repeating each simulation scenario to ensure that the masked results of

repeated runs are consistent. Such a consistency indicates that the number of flows in a scenario is adequate for the given thresholds to indicate likelihood (de' Michieli Vitturi and Tarquini 2018).

Another caveat with our strategy was that there was no existing procedure for uncertainty testing of input parameters, nor did we have a template of how we wished to communicate the uncertainties of the model results. In order to evaluate the uncertainty of the input parameters themselves, statistical tools such as Dakota (Adams et al., 2021), specifically designed to perform sensitivity analysis and uncertainty quantification with existing numerical codes, could be used. This would allow to assess the most critical input parameters and develop map layers to communicate the uncertainty of the parameter space.

area

Finally, updating the computational domain through incorporation of ancillary data such as syn-eruptive DEMs or lava thickness maps in lava simulations have been thought of as a route to improve lava flow simulations bypassing caveats of lava simulation codes to reproduce the lava flow fields more consistently (Harris et al., 2016, Tarquini et al., 2018).

However, as we discovered, updating the topographic domain created a new problem: namely the restart problem described in 4.2.2, where the real eruption was continuously transporting lava to the edges of the flow-field while the re-initialized simulation experienced a delay in the lava field expansion as the simulation required a „spin up time" to get lava advancing at the edges. We have learned that discretizing lava simulations into sequential separate simulations with updated topography will require a strategy to deal with this "spin up time". This issue is not specific to the MrLavaLoba code but will likely apply to all lava simulation codes that attempt to sequentially introduce new starting conditions to implement time evolution.

We propose some potential ways forward to solve this:

1) integrate lava transport system

2) Find a way of having a „spin up" that will re-establish activity at the flow field edges.

3) Implement additional sources at active lava margins as we did for the worst-case scenario runs described in 4.2.3.

5.3 Improved dissemination strategies Dissemination: Communication & Hazard maps

During this prolonged volcanic crisis, delivering information on lava flow hazard assessment was a complicatedcomplicated task and identifying a good strategyies to do it was a learning process. Two main elements were eventually considered when designing map layouts and content: (a) which kind of stakeholders would receive the information and which role did they hadhave during in responding to the crisis (e.g., experts, civil defense/responders, decision makers or the general public) and (b) which information they needed to receive to fulfill their operations and tasks. During the eruption regular and frequent meetings were held between monitoring personnel on duty, scientists, Civil protection representatives, local police and rangers who were patrolling the area. For the first months they were held on a daily basisdaily, and eventually they held were bi-weekly. Lava flow invasion maps were shown and discussed at these

briefings (Barsotti et al. 2023), as well as during dedicated meetings and ~~. Occasionally, lava flow hazard maps~~ were occasionally reiterated ~~upon comments and~~based on feedback provided by the users.

Thanks to this interaction with the stakeholders, it became clear that the main products for them were the short-term scenarios, ~~and the~~ short-term worst-case scenarios (Fig.7) and the long-term scenarios (Fig.10). The maps were prepared by following three main criteria: (~~1~~a) simple maps showing potential lava inundation areas, and not lava thicknesses, (~~2~~b) showing the uncertainty related to the model results, and (~~3~~c) including all ~~necessary information to understand the results by avoiding figure captions, so that~~ key- information (e.g., name of lava simulation model, key input parameters, time-frame and main assumptions) to ~~could not be inadvertently separated from the shared results and therefore the~~ensure that final product would be self-explaining, even if a figure caption inadvertently was separated from the map. Thus, we were~~P~~ providing multiple map products and customizing them to user needs is in accordance with volcano observatory best practices workshops (Pallister et al., 2019, Lowenstern et al., 2022). Distributing maps for the public was complicated and required several iterations and double-checking from experts, to avoid that results triggered many questions and alarmed the community (See e.g., maps ~~In some instances, maps were~~ made publicly available on the Icelandic Meteorological office~~IMO~~'s web-site ~~for a wider distribution with the general public and journalists being the main receivers~~: ~~(~~https://www.vedur.is/um-vi/frettir/vel-fylgst-med-skjalftahrinunni-vid-keili and https://www.vedur.is/um-vi/frettir/hraunflaedilikon-hafa-sannad-sig-i-eldgosinu-vid-fagradalsfjall)~~. Distributing maps for a larger and less educated audience was even more complicated and this task was not done prior several iterations and double-checking, as the results could have triggered many questions and alarmed the community~~. ~~Providing multiple map products and customizing them to user needs is in accordance with volcano observatory best practices workshops (Pallister et al., 2019, Lowenstern et al., 2022)~~

~~Based on the bi-weekly meetings with stakeholders it became clear that efficient lava flow simulations and dissemination of results relied on understanding the needs of the stakeholders: (a) what information did they want or need (e.g., inundated area, time frames of processes), (b) who are they and what is their level of engagement with the material (e.g., experts, civil defence~~defense~~/responders, decision makers or the general public) and (c) what type of product/map would be best understood given what was known about (a) and (b). For the eruption at Fagradalsfjall 2021 maps were developed as the crisis continued and as feedback was received from the stakeholders in regular meetings. The main products were short-term more-likely scenarios, short-term worst-case scenarios (Fig.~~7~~5) and long-term scenarios (Fig.~~10~~8).~~

~~In our case of a long-lasting volcanic crisis, the information had has to be communicated in brief and efficient meetings with the agencies responsible for the operations, as well as during some ad-hoc meetings with key stakeholders, dedicated to discuss the most important results shown in the lava flow maps. It turned out the most efficient way to communicate results were (1) simple maps that showed potential lava inundation areas, and not lava thicknesses, (2) to have uncertainty related to~~

the model results included on the maps, and (3) that all necessary information to understand the results have to be on the map (as opposed to in a figure caption, for example), so that key- information (e.g., name of lava simulation model, key input parameters, time-frame and main assumptions) could not be inadvertently separated from the shared results and therefore the final product would be self-explaining.

As described above (section 5.1 and 5.2) including the uncertainty of the lava simulation results, required changes to the simulation code, and in the modelling approach, which, to begin with was requiring extra time. However, it also became clear that if when we had efficient ways to include uncertainty in the simulation results, the modeler could (ia) avoid time-consuming fine tuning of input parameters, (iib) save time in the map production and (iiic) be much more efficient in communicating the results in a consistent way.

For the next volcanic crisis, we aimthe goal is to have pre-made-formatted map templates for short-term scenarios, short-term worst-case scenarios and the long-term scenarios similar to Fig. 7, 8 and 10. These should be developed collaboratively with hazard and cartography experts to help the lava flow modelers to find a suitable balance between essential information and simplicityreadability. Secondly, an explanation of the lava hazard modelling approach should be prepared in multiple languages to accompany the maps in the stakeholder meetingswhen communicatedion to the public. Finally, it would be helpful to discriminate between design of map products delivered to (a1) scientific community, (2b) stakeholders and (c3) the general public and potentially set-up some a priori agreements about what type of results should be disseminated to each group and consider appropriate the platform for such information (websites, web map servicesms, social media).

6 Conclusions (Sara to here)

On March 19 to September 18, 2021, the first eruption in ca. 800 years took place on the Reykjanes Peninsula, Iceland. Being lLocated in the backyard of the capital Reykjavík and the international airport, this effusive eruption was the most visited eruption in Iceland to date and needed intense monitoring and thorough lava hazard assessment. The eruption harmed no critical infrastructure Furthermore, itand became a test case study for the monitoring and hazard assessment for future eruptions on the Peninsula that can have a greater societal impact issuing lava into inhabited areas or inundate essential infrastructure.

In this study we documented how various lava flow simulation strategies using the stochastic code MrLavaLoba was a useful and a flexible toolwere used to evaluate hazards during the 6-month long effusive event. Different lava simulation strategies were deployed during the unrest and eruption depending on purpose of simulation. and their Ooverall, the purposes were three-fold:: (a) pre-eruption simulations to investigate potential exposure of critical infrastructure in immediate danger forto lava flow inundation, based on location of deformation signal (b) Simulations simulations addressing areas of short-term

(weeks) lava ~~danger for lava flow inundation~~hazards and worst-case scenarios ~~(Two weeks)~~ and (c) simulations addressing ~~areas of danger for lava flow inundation in~~ long-term (~~Months~~ months to years) lava hazards.

~~The functionalities of the code made it flexible and possible to implement it for multiple purposes. Unique to other stochastic codes,~~ MrLavaLoba ~~includes lava volume~~provides~~,~~ final lava extent, ~~it produces~~ lava thickness layers and it continually modifies the topography during the simulation~~it changes updates the topography during the simulation~~. This was very important during the Fagradalsfjall 2021 crisis because the ~~hazards related to the nested valley systems that were~~ timing of the filling and spilling from one valley to another could not have been addressed by codes not including lava volume. ~~Furthermore, i~~It is very easy to implement topographic changes, e.g., by implementing lava flow thickness maps obtained during the eruption or lava barriers, a key functionality of the code that made it suitable for testing suggested and built lava barriers ~~which were key for testing suggested and build lava barriers~~. As the eruption got more complex, weaknesses of the lava flow simulation came into light. Some input parameters required time-consuming tuning when the spatial resolution of the runs was changed, a restart problem related to step-wise simulations with updated topography caused delayed activation of lava flow margins, and challenges relating to time-evolving changes in eruption style.

~~Tuning of the input parameters needed for the MrLavaLoba code was at times time-consuming, especially during changes in changeable eruptive activity or changes in terrain and ideally tuning of a greater number of eruptive scenarios in different terrain has to be prepared beforehand. A couple of other issues discovered during the crisis was the restart problem when updating the topographic computational domain. After updating the topography and restarting the lava flow simulation a delay in the lava field expansion were~~was observed in the simulated lava field while the real eruption continuously were ~~was transporting lava to the edges. Another issue discussed was the scaling issues caused by changing spatial resolution of the computational domain.~~

During the crisis the code was improved ~~was updated~~ to increase functionalities ~~such as~~ including multiple eruption vents simultaneously and produce multiple lava thickness masks. The former was important during the vent migration phase, while the latter was necessary to communicate uncertainty in model results.

Future scientific improvements could include strategies to automate quantitative evaluations of model results, quantitative uncertainty analysis of input parameters and prepared map templates to efficiently disseminate results.

~~Future improvements of the code and developed approaches include strategies to make (i) quantitative evaluation strategy of modelling results that can be used during the crisis (ii) establish uncertainty testing of input parameters and (iii) make map templates to efficiently disseminate results.~~

The lava flow model results were shared regularly with the scientific community, the agencies responsible for the operations in-situ and to the ~~general public~~public (through news articles on institutions websites). The numerical code and the established modelling procedures are considered to have been very successful for responding to an eruption that called to

tourists and visitors from all over the world.~~Regardless the multiple issues, challenges and open questions listed in this review, the numerical code and the established modelling procedures were considered very successful for responding to an eruption that called tourists and visitors from all over the world.~~

7 Code and Data availability

MrLavaLoba is code was published in 2018 (de'' Michieli Vitturi and Tarquini, 2018) and is freely available at the model repository (http://demichie.github.io/MrLavaLoba/). Relevant data for this study can be found in Pedersen et al. (2022b), https://doi.org/10.5281/zenodo.6581470. The outputs of MrLavaLoba simulations are available upon request to the corresponding author.

Author contributions

GBMP undertook manuscript preparation, model implementation, strategy development, validation, and formal analysis, and communication with stakeholders. MAP undertook the background research, model implementation for pre-eruption runs, formal analysis, communication with stakeholders and review of manuscript. SB undertook the background research, supervised strategy development and stakeholder contact and review of the manuscript. ST and MdMV developed the code, supervised strategy development and code implementation and reviewed the manuscript. BÓ undertook the background research and reviewed the manuscript and RHÞ contributed to map production and review of the manuscript.

Competing interests

The contact author has declared that neither they nor their co-authors have any competing interests.

Acknowledgements

The authors would like to acknowledge scientists and stakeholders providing feedback on the communication of hazard maps during stakeholder meetings. Furthermore, they would like to thank an anonymous reviewer as well as Freysteinn Sigmundsson who provided an image of the eruption used in figure 5. Finally, we would like to thank our ~~their~~ financial support.

Formatted: Underline, Highlight

Financial support

This research has been supported by the Icelandic Research ~~fund,~~fund; Grant No. 206755-052 awarded to GBMP.

References

Adams, B.M., Bohnhoff, W.J., Dalbey, K.R., Ebeida, M.S., Eddy, J.P., Eldred, M.S., Hooper, R.W., Hough, P.D., Hu, K.T., Jakeman, J.D., Khalil, M., Maupin, K.A., Monschke, J.A., Ridgway, E.M., Rushdi, A.A., Seidl, D.T., Stephens, J.A., Swiler, L.P., and Winokur, J.G.: Dakota, A Multilevel Parallel Object-Oriented Framework for Design Optimization, Parameter Estimation, Uncertainty Quantification, and Sensitivity Analysis: Version 6.15 User's Manual, Sandia Technical Report SAND2020-12495, November 2021.

Andrésdóttir, Þ. B.: Eldfjallavá á Reykjanesi, Thesis, 2016.

Andrésdóttir, Þ. B.: Volcanic hazard and risk assessment at Reykjanes, vulnerability of infrastructure, Thesis, 2018.

Barberi, F. and Villari, L.: Volcano monitoring and civil protection problems during the 1991–1993 Etna eruption. Acta Vulcanologica, 4, 157-165, 1994.

Barsotti, S., Parks, M. M., Pfeffer, M. A., Óladóttir, B. A., Barnie, T., Titos, M. M., Jónsdóttir, K., Pedersen, G. B. M., Hjartardóttir, Á. R., Stefansdóttir, G., Johannsson, T., Arason, Þ., Gudmundsson, M. T., Oddsson, B., Þrastarson, R. H., Ófeigsson, B. G., Vogfjörd, K., Geirsson, H., Hjörvar, T., von Löwis, S., Petersen, G. N., and Sigurðsson, E. M.: The eruption in Fagradalsfjall (2021, Iceland): how the operational monitoring and the volcanic hazard assessment contributed to its safe access, Nat Hazards, 116, 3063–3092, https://doi.org/10.1007/s11069-022-05798-7, 2023.

~~Barsotti, S., Parks, M. M., Pfeffer, M. A. et al. The Eruption in Fagradalsfjall (2021, Iceland): How The Operational Monitoring and The Volcanic Hazard Assessment Contributed to Its Safe Access, 28 March 2022, PREPRINT (Version 1) available at Research Square [https://doi.org/10.21203/rs.3.rs-1453832/v1]~~

Belart, J. M. C., Magnússon, E., Berthier, E., Pálsson, F., Aðalgeirsdóttir, G., and Jóhannesson, T.: The geodetic mass balance of Eyjafjallajökull ice cap for 1945-2014: processing guidelines and relation to climate. J. Glaciol. 65, 395–409. Doi: 10.1017/jog.2019.16, 2019.

Cappello, A., Ganci, G., Calvari, S., Pérez, N. M., Hernández, P. A., Silva, S. V., Cabral, J., and Del Negro, C.: Lava flow hazard modeling during the 2014–2015 Fogo eruption, Cape Verde. Journal of Geophysical Research: Solid Earth, 121(4), 2290–2303. https://doi.org/10.1002/2015JB012666, 2016a.

Cappello, A., Hérault, A., Bilotta, G., Ganci, G., and Del Negro, C.: MAGFLOW: a physics-based model for the dynamics of lava-flow emplacement, Geological Society, London, Special Publications, 426, 357–373, https://doi.org/10.1144/SP426.16, 2016b.

Carracedo, J. C., Troll, V. R., Day, J. M. D., Geiger, H., Aulinas, M., Soler, V., Deegan, F. M., Perez-Torrado, F. J., Gisbert, G., Gazel, E., Rodriguez-Gonzalez, A., and Albert, H.: The 2021 eruption of the Cumbre Vieja volcanic ridge on La Palma, Canary Islands, Geology Today, 38, 94–107, https://doi.org/10.1111/gto.12388, 2022.

Chevrel, M. O., Favalli, M., Villeneuve, N., Harris, A. J. L., Fornaciai, A., Richter, N., Derrien, A., Boissier, P., Di Muro, A., and Peltier, A.: Lava flow hazard map of Piton de la Fournaise volcano, Natural Hazards and Earth System Sciences, 21, 2355–2377, https://doi.org/10.5194/nhess-21-2355-2021, 2021.

Chevrel, M. O., Labroquère, J., Harris, A. J. L., and Rowland, S. K.: PyFLOWGO: An open-source platform for simulation of channelized lava ~~therm~~30hermoso-rheological properties. Computers & Geosciences, 111, 167–180. https://doi.org/10.1016/j.cageo.2017.11.009, 2018.

Clifton, A. E., and Kattenhorn, S. A.: Structural architecture of a highly oblique divergent plate boundary segment. Tectonophysics, 419(1), 27–40. https://doi.org/10.1016/j.tecto.2006.03.016, 2006.

Cubuk-Sabuncu, Y., Jónsdóttir, K., Caudron, C., Lecocq, T., Parks, M. M., Geirsson, H., and Mordret, A.: Temporal Seismic Velocity Changes During the 2020 Rapid Inflation at Mt. Þorbjörn-Svartsengi, Iceland, Using Seismic Ambient Noise, Geophysical Research Letters, 48, e2020GL092265, https://doi.org/10.1029/2020GL092265, 2021.

de' Michieli Vitturi, M., and Tarquini, S.: MrLavaLoba: A new probabilistic model for the simulation of lava flows as a settling process. Journal of Volcanology and Geothermal Research, 349, 323–334. https://doi.org/10.1016/j.jvolgeores.2017.11.016, 2018.

Dietterich, H. R., Lev, E., Chen, J., Richardson, J. A., and Cashman, K. V.: Benchmarking computational fluid dynamics models of lava flow simulation for hazard assessment, forecasting, and risk management. Journal of Applied Volcanology, 6(1), 9. https://doi.org/10.1186/s13617-017-0061-x, 2017.

Formatted: English (United States)

Formatted: Not Highlight

Formatted: Highlight

Formatted: Not Highlight

Formatted: Not Highlight

Eibl, E. P. S., Thordarson, T., Höskuldsson, Á., Gudnason, E. Á., Dietrich, T., Hersir, G. P., and Ágústsdóttir, T.: Evolving shallow conduit revealed by tremor and vent activity observations during episodic lava fountaining of the 2021 Geldingadalir eruption, Iceland, Bull Volcanol, 85, 10, https://doi.org/10.1007/s00445-022-01622-z, 2023.

Einarsson, P., Hjartardóttir, Á. R., Hreinsdóttir, S., and Imsland, P.: The structure of seismogenic strike-slip faults in the eastern part of the Reykjanes Peninsula Oblique Rift, SW Iceland. Journal of Volcanology and Geothermal Research, 391, 106372. https://doi.org/10.1016/j.jvolgeores.2018.04.029, 2020.

Einarsson, P., and Sæmundsson, K.: Earthquake epicenters 1982-1985 and volcanic systems in Iceland = Upptok jardskjalfta 1982-1985 og eldstodvakerfi a Islandi [Map]. Menningarsjóður, 1987.

Einarsson, S.: Brennisteinsfjöll Alternative name: Bláfjöll, in: Catalogue of Icelandic volcanoes, edited by: Óladóttir, B. A., Larsen, G., and Gudmundsson, M. T., IMO, UI and CPD-NCIP, Retrieved from http://icelandicvolcanoes.is/?volcano=BRE#, 2019a.

Einarsson, S.: Krýsuvík-Trölladyngja Alternative name: Krísuvík, in: Catalogue of Icelandic volcanoes, edited by: Óladóttir, B. A., Larsen, G., and Gudmundsson, M. T., IMO, UI and CPD-NCIP, Retrieved from http://icelandicvolcanoes.is/?volcano=KRY#, 2019b.

Favalli, M., Pareschi, M. T., Neri, A., and Isola, I.: Forecasting lava flow paths by a stochastic approach. Geophysical Research Letters, 32(3). https://doi.org/10.1029/2004GL021718, 2005.

Favalli, M., Tarquini, S., Papale, P., Fornaciai, A., and Boschi, E.: Lava flow hazard and risk at Mt. Cameroon volcano, Bull Volcanol, 74, 423–439, https://doi.org/10.1007/s00445-011-0540-6, 2012.

Felpeto, A., Martí, J., and Ortiz, R.:Automatic GIS-based system for volcanic hazard assessment. Journal of Volcanology and Geothermal Research, 166, 106-116. Doi:10.1016/j.jvolgeores.2007.07.008, 2007.

Flóvenz, Ó. G., Wang, R., Hersir, G. P., Dahm, T., Hainzl, S., Vassileva, M., Drouin, V., Heimann, S., Isken, M. P., Gudnason, E. Á., Ágústsson, K., Ágústsdóttir, T., Horálek, J., Motagh, M., Walter, T. R., Rivalta, E., Jousset, P., Krawczyk, C. M., and Milkereit, C.: Cyclical geothermal unrest as a precursor to Iceland's 2021 Fagradalsfjall eruption. Nature Geoscience, 15(5), 397–404. https://doi.org/10.1038/s41561-022-00930-5, 2022.

Ganci, G., Vicari, A., Cappello, A., & Del Negro, C.: An emergent strategy for volcano hazard assessment: From thermal satellite monitoring to lava flow modeling. Remote Sensing of Environment, 119, 197–207. https://doi.org/10.1016/j.rse.2011.12.021, 2012.

Gee, M. A. M.: Volcanology and geochemistry of Reykjanes Peninsula: Plume-mid-ocean ridge interaction. [PhD]. University of London, 1998.

~~Geirsson, H., Parks, M. M., Vogfjörd, K., Einarsson, P., Sigmundsson, F., Jónsdóttir, K., Drouin, V., Ófeigsson, B. G., Hreinsdóttir, S., and Ducrocq, C.: The 2020 volcano-tectonic unrest at Reykjanes Peninsula, Iceland: stress triggering and reactivation of several volcanic systems, https://doi.org/10.5194/egusphere-egu21-7534, EGU General Assembly 2021.~~

Glaze, L. S., and Baloga, S. M.: Simulation of inflated pahoehoe lava flows. Journal of Volcanology and Geothermal Research, 255, 108–123. https://doi.org/10.1016/j.jvolgeores.2013.01.018, 2013.

Greenfield, T., Winder, T., Rawlinson, N., Maclennan, J., White, R. S., Ágústsdóttir, T., Bacon, C. A., Brandsdóttir, B., Eibl, E. P. S., Glastonbury-Southern, E., Gudnason, E. Á., Hersir, G. P., and Horálek, J.: Deep long period seismicity preceding and during the 2021 Fagradalsfjall eruption, Iceland, Bull Volcanol, 84, 101, https://doi.org/10.1007/s00445-022-01603-2, 2022.

Harris, A. J., and Rowland, S.: FLOWGO: A kinematic ~~thermo~~31hermos-rheological model for lava flowing in a channel. Bulletin of Volcanology, 63(1), 20–44. https://doi.org/10.1007/s004450000120, 2001.

Harris, A. J. L., Villeneuve, N., Di Muro, A., Ferrazzini, V., Peltier, A., Coppola, D., Favalli, M., Bachèlery, P., Froger, J.-L., Gurioli, L., Moune, S., Vlastélic, I., Galle, B., and Arellano, S.: Effusive crises at Piton de la Fournaise 2014-2015: a review of a multi-national response model. Journal of Applied Volcanology, 6(1), 11. https://doi.org/10.1186/s13617-017-0062-9, 2017.

Harris, A.J.L., Chevrel, M. O., Coppola, D., Ramsey, M. S., Hrysiewicz, A., Thivet, S., Villeneuve, N., Favalli, M., Peltier, A., Kowalski, P., DiMuro, A., Froger, J.-L., and Gurioli, L.: Validation of an integrated satellite-data-driven response to

Formatted: Not Highlight

an effusive crisis: the April–May 2018 eruption of Piton de la Fournaise. Annals of Geophysics, 61. https://doi.org/10.4401/ag-7972, 2019.
Jakobsson, S. P., Jónsson, J., and Shido, F.: Petrology of the Western Reykjanes Peninsula, Iceland. Journal of Petrology, 19(4), 669–705. https://doi.org/10.1093/petrology/19.4.669, 1978.
Jones, J. G.: Intraglacial volcanoes of the Laugarvatn region, south-west Iceland—I. Quarterly Journal of the Geological Society, 124(1–4), 197–211. https://doi.org/10.1144/gsjgs.124.1.0197, 1969.
Jónsson, J.: Jarðfræðikort af Reykjanesskaga (Geological map of the Reykjanes Peninsula). Orkustofnun Jarðhitadeilsd 7831, 1978.
Jóhannesson, T., Björnsson, H., Magnusson, E., Gudmundsson, S., Palsson, F., Sigurdsson, O., Throsteinsson, Th. And Berthier, E.: Ice-volume changes, bias estimation of mass-balance measurements and changes in subglacial lakes derived by lidar mapping of the surface of ~~icelandi~~32hermos32nc glaciers. Annals of Glaciology, 54 (63), 63–74, 2013.
Kauahikaua, J.: Lava flow hazard assessment, as of August 2007, for Kilauea east rift zone eruptions, Hawaii island. U.S. Geological Survey Open-File Report 2007-1264, August, 9 p. http://www.usgs.gov/pubprod, 2007.
Klein, F. W., Einarsson, P., and Wyss, M.:The Reykjanes Peninsula, Iceland, earthquake swarm of September 1972 and its tectonic significance. Journal of Geophysical Research (1896-1977), 82(5), 865–888. https://doi.org/10.1029/JB082i005p00865, 1977.
Lowenstern, J. B., Wallace, K., Barsotti, S., Sandri, L., Stovall, W., Bernard, B., Privitera, E., Komorowski, J.-C., Fournier, N., Balagizi, C., and Garaebiti, E.: Guidelines for volcano-observatory operations during crises: recommendations from the 2019 volcano observatory best practices meeting, Journal of Applied Volcanology, 11, 3, https://doi.org/10.1186/s13617-021-00112-9, 2022
Martí, J., Becerril, L., and Rodríguez, A.: How long-term hazard assessment may help to anticipate volcanic eruptions: The case of La Palma eruption 2021 (Canary Islands), Journal of Volcanology and Geothermal Research, 431, 107669, https://doi.org/10.1016/j.jvolgeores.2022.107669, 2022.
Mossoux, S., Saey, M., Bartolini, S., Poppe, S., Canters, F., and Kervyn, M.: Q-LAVHA: A flexible GIS plugin to simulate lava flows. Computers & Geosciences, 97, 98–109. https://doi.org/10.1016/j.cageo.2016.09.003, 2016.
Neal, C. A., Brantley, S. R., Antolik, L., Babb, J. L., Burgess, M., Calles, K., Cappos, M., Chang, J. C., Conway, S., Desmither, L., Dotray, P., Elias, T., Fukunaga, P., Fuke, S., Johanson, I. A., Kamibayashi, K., Kauahikaua, J., Lee, R. L., Pekalib, S., … Damby, D.: The 2018 rift eruption and summit collapse of Kīlauea Volcano. Science, 363(6425), 367–374. https://doi.org/10.1126/science.aav7046, 2019.
Óladóttir, B. A., Óladóttir, B. A., Larsen, G., and Gudmundsson, M. T.: Fagradalsfjall Also known as part of Krýsuvík-Trölladyngja volcanic system, in: Catalogue of Icelandic volcanoes, IMO, UI and CPD-NCIP, Retrieved from http://icelandicvolcanoes.is/?volcano=FAG#, 2022.
Pallister, J., Papale, P., Eichelberger, J., Newhall, C., Mandeville, C., Nakada, S., Marzocchi, W., Loughlin, S., Jolly, G., Ewert, J., and Selva, J.: Volcano observatory best practices (VOBP) workshops—A summary of findings and best-practice recommendations. Journal of Applied Volcanology, 8(1), 2. https://doi.org/10.1186/s13617-019-0082-8, 2019.
Pedersen, G. B. M., and Grosse, P.: Morphometry of subaerial shield volcanoes and glaciovolcanoes from Reykjanes Peninsula, Iceland: Effects of eruption environment. Journal of Volcanology and Geothermal Research, 282, 115–133. https://doi.org/10.1016/j.jvolgeores.2014.06.008, 2014.
Pedersen, G. B. M., Belart, J. M. C. Óskarsson, B. V., Gudmundsson, M. T., Gies, N., Högnadóttir, Th., Hjartardóttir, A. R., Pinel, V., Berthier, E., Dürig, T., Reynolds, H. I., Hamilton, C. W., Valsson, G., Einarsson, P., Ben-Yehosua, D., Gunnarsson, D., Oddsson, B.: Volume, effusion rate, and lava transport during the 2021 Fagradalsfjall eruption: Results from near real-time photogrammetric monitoring. Geophisical Research Letters, ~~DOI~~doi:10.1029/2021GL097125, ~~in press~~2022a.
Pedersen, G. B. M., Belart, J. M.C., Óskarsson, B. V., Gudmundsson, M. T., Gies, N., Högnadóttir, Th., Hjartadótti, Á. R. Pinel, V., Berthier, E., Dürig, T., Reynolds, H. I., Hamilton, C. W., Valsson, G., Einarsson, P., Ben-Yehosua, D., Gunnarsson, A., and Oddsson, B.: Digital Elevation Models, orthoimages and lava outlines of the 2021 Fagradalsfjall eruption: Results from near real-time photogrammetric monitoring (Version v1) [Data set]. Zenodo. https://doi.org/10.5281/zenodo.6581470, 2022b.
Peltier, A., Ferrazzini, V., Di Muro, A., Kowalski, P., Villeneuve, N., Richter, N., Chevrel, M. O., Froger, J.-L., and Hrysiewicz A, Gouhier M, Coppola D, Retailleau L, Beauducel F, Boissier P, Brunet C, Catherine P, Fontaine F, Lauret

F, Garavaglia L, Lebreton J, Canjamale K, Desfete N, Griot C, Arellano S and Liuzzo M, G. S.: Volcano crisis management during COVID-19 lockdown at Piton de la Fournaise (La Réunion). Seismological Research Letters, On line No, 1–15. https://doi.org/10.1785/0220200212, 2020.

Peltier, A, Chevrel, M. O., Harris, A. J. L., and Villeneuve, N.: Reappraisal of gap analysis for effusive crises at Piton de la Fournaise. Journal of Applied Volcanology, 11(1), 1–17. https://doi.org/10.1186/s13617-021-00111-w, 2022.

Pfeffer, M. A., Barsotti, S., Karlsdóttir, S., Jensen, E. H., Pagneux, E. P., Björnsson, B. B., Jóhannesdóttir, G., Höskuldsson, Á., Sandri, L., Selva, J., and Tarquini, S.: An initial volcanic hazard assessment of the Vestmannaeyjar Volcanic System. Icelandic Meterological Office, Iceland, 73 pp., 2020.

Pierrot Deseilligny, M., and Clery, I.: Apero, an open source bundle ~~adjusment~~adjustment software for automatic calibration and orientation of set of images. Int. Arch. Photogr. Remote Sens. Spat. Inform. Sci. 3816, 269–276. Doi: 10.5194/isprsarchives-XXXVIII-5-W16-269-2011, 2011.

Porter, C., Morin, P., Howat, I., Noh, M.-J., Bates, B., Peterman, K., et al.: ArcticDEM. Harvard Dataverse, V1. Polar Geospatial Center, University of Minnesota. Doi: 10.7910/DVN/OHHUKH, 2018.

Richter, N., Favalli, M., de Zeeuw-van Dalfsen, E., Fornaciai, A., da Silva Fernandes, R. M., Pérez, N. M., Levy, J., Victória, S. S., and Walter, T. R.: Lava flow hazard at Fogo Volcano, Cabo Verde, before and after the 2014–2015 eruption, Natural Hazards and Earth System Sciences, 16, 1925–1951, https://doi.org/10.5194/nhess-16-1925-2016, 2016.

Rossi, M. J.: Morphology and mechanism of eruption of postglacial shield volcanoes in Iceland. Bulletin of Volcanology, 57(7), 530–540. https://doi.org/10.1007/BF00304437, 1996.

Rupnik, E., Daakir, M., and Pierrot Deseilligny, M.: MicMac—- a free, open-source solution for photogrammetry. Open Geospatial Data Softw. Stand. 2:14. Doi: 10.1186/s40965-017-0027-2, 2017.

Sigmundsson, F., Parks, M., Hooper, A., Geirsson, H., Vogfjörd, K. S., Drouin, V., Ófeigsson, B. G., Hreinsdóttir, S., Hjaltadóttir, S., Jónsdóttir, K., Einarsson, P., Barsotti, S., Horálek, J., and Ágústsdóttir, T.: Deformation and seismicity decline before the 2021 Fagradalsfjall eruption, Nature, 609, 523–528, https://doi.org/10.1038/s41586-022-05083-4, 2022.

Sigurgeirsson, M. A. and Einarsson, S.: Reykjanes and Svartsengi volcanic systems. In: Oladottir, B., Larsen, G. and Guðmundsson, M. T.: Catalogue of Icelandic Volcanoes. IMO, UI and CPD-NCIP. Retrieved from http://icelandicvolcanoes.is/?volcano=REY#, 2016.

Sæmundsson, K.: Hengill, in: Catalogue of Icelandic volcanoes, edited by: Óladóttir, B. A., Larsen, G., and Gudmundsson, M. T., IMO, UI and CPD-NCIP, Retrieved from http://icelandicvolcanoes.is/?volcano=HEN#, 2019.

Sæmundsson, K., Jóhanneson, H., Hjartarson, Á., Kristinsson, S. G., & Sigurgeirsson, M. Á.: Geologic map of Southwest Iceland. [Map]. Iceland Geosurvey, 2010.

Sæmundsson, K. and Sigurgeirsson, M. Á.: Reykjanesskagi, in: Náttúruvá, edited by: Sólnes, J., Sigmundsson, F., and Bessason, B., Viðlagatrygging Íslands / Háskólaútgáfa, 379–401, 2013.

Sæmundsson, K., Sigurgeirsson, M. Á., and Friðleifsson, G. Ó.: Geology and structure of the Reykjanes volcanic system, Iceland. Journal of Volcanology and Geothermal Research, 391, 106501, 2020. https://doi.org/10.1016/j.jvolgeores.2018.11.022, 2020.

Tarquini, S., and Favalli, M.: Uncertainties in lava flow hazard maps derived from numerical simulations: The case study of Mount Etna. Journal of Volcanology and Geothermal Research, 260, 90–102. https://doi.org/10.1016/j.jvolgeores.2013.04.017, 2013.

Tarquini, S., Vitturi, M. de' M., Jensen, E., Pedersen, G., Barsotti, S., Coppola, D., and Pfeffer, M. A.: Modeling lava flow propagation over a flat landscape by using MrLavaLoba: The case of the 2014–2015 eruption at Holuhraun, Iceland. Annals of Geophysics, 62(2), VO228–VO228. https://doi.org/10.4401/ag-7812, 2019.

Thorkelsson, B. (ed.): The 2010 Eyjafjallajökull eruption, Iceland. Report to ICAO – June 2012. Icelandic Meteorological Office, University of Iceland. Institute of Earth Sciences, The National Commissioner of the Icelandic Police, Reykjavík. IVATF 4-IP/3, 206 s. Steering and editorial committee: Sigrún Karlsdóttir (chair), Ágúst Gunnar Gylfason, Ármann Höskuldsson, Bryndís Brandsdóttir, Evgenia Ilyinskaya, Magnús Tumi Guðmundsson and Þórdís Högnadóttir, 2012.

Vicari, A., Ganci, G., Behncke, B., Cappello, A., Neri, M., and Del Negro, C.: Near-real-time forecasting of lava flow hazards during the 12–13 January 2011 Etna eruption. Geophysical Research Letters, 38(13). https://doi.org/10.1029/2011GL047545, 2011.

Field Code Changed

Wright, R., Garbeil, H., and Harris, A. J. L.: Using infrared satellite data to drive a ~~therm~~ 34hermos~~o~~-rheological/stochastic lava flow emplacement model: A method for near-real-time volcanic hazard assessment. Geophysical Research Letters, 35(19), 1–5. https://doi.org/10.1029/2008GL035228, 2008.

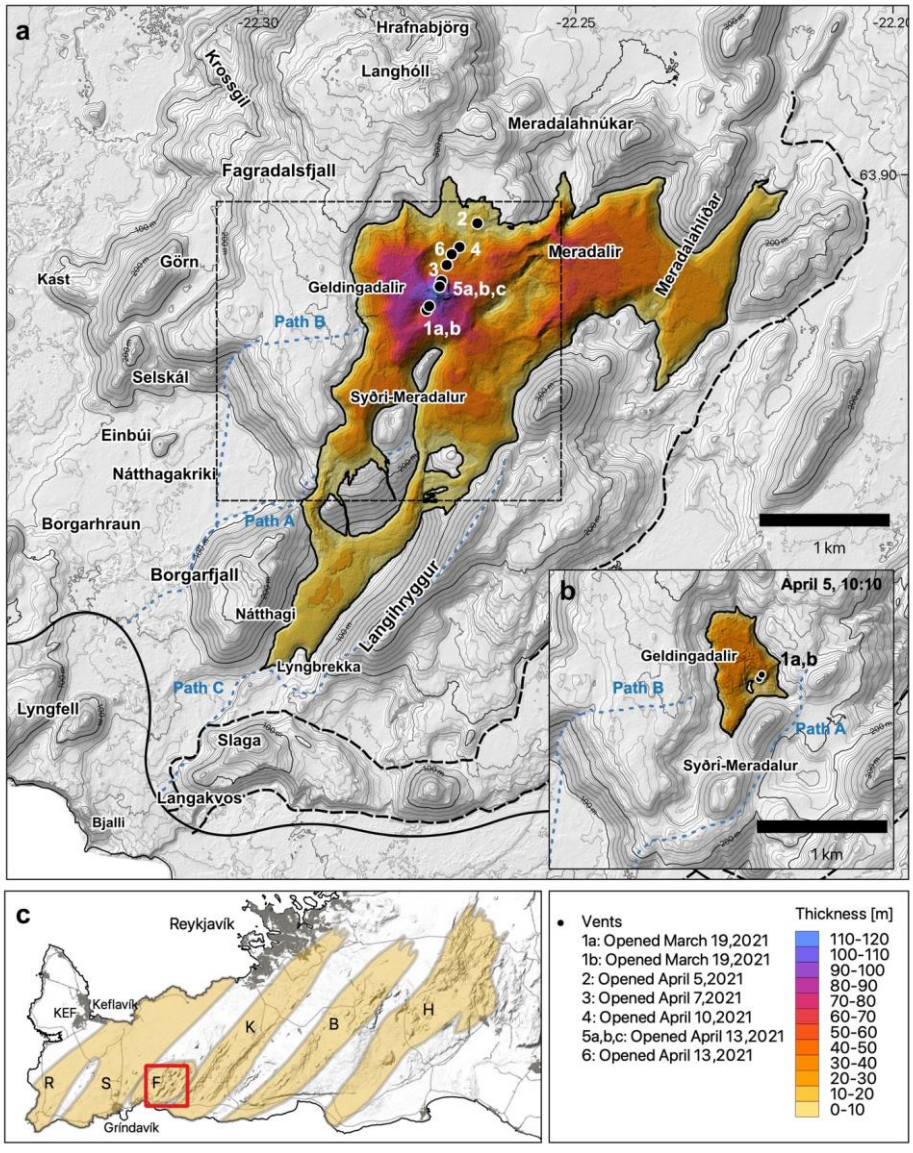
a
-22.30
-22.25
Hrafnabjörg
Langhóll
Krossgil
Meradalahnúkar
Fagradalsfjall
63.90
2
6
4
3
5a,b,c
1a,b
Meradalir
Meradalahlíðar
Geldingadalir
Görn
Kast
Path B
Selskál
Syðri-Meradalur
Einbúi
Nátthagakriki
Borgarhraun
Path A
1 km
Borgarfjall
Nátthagi
Langihryggur
Lyngbrekka
Path C
Lyngfell
Slaga
Langakvos
Bjalli
b
April 5, 10:10
Geldingadalir
1a,b
Path B
Path A
Syðri-Meradalur
1 km
c
Reykjavík
Keflavík
KEF
K
B
H
R
S
F
Grindavík
Vents
1a: Opened March 19,2021
1b: Opened March 19,2021
2: Opened April 5,2021
3: Opened April 7,2021
4: Opened April 10,2021
5a,b,c: Opened April 13,2021
6: Opened April 13,2021
Thickness [m]
110-120
100-110
90-100
80-90
70-80
60-70
50-60
40-50
30-40
20-30
10-20
0-10

Figure 1: a) Overview of the Fagradalsfjall area at the end of the eruption. Vents are marked with dots and numbered chronologically after opening time. Lava thickness map is from September 30, 2021 (Pedersen et al., 2022b). Dashed black box indicates the extent of frame b. b) Overview of the Fagradalsfjall area by the end of ~~the~~ Phase 1. Lava thickness map is from April 5, 2021 (Pedersen et al., 2022b). Hiking paths are shown in dashed blue. C) Map of the Reykjanes Peninsula. The red box indicates the area displayed in a). Densely populated areas are marked in gray. Volcanic systems (Sæmundsson and Sigurgeirsson, 2013, fig. 4.13.1) are marked ~~with~~ orange and denoted by capital letters according to their name; R: Reykjanes, S: Svartsengi, F: Fagradalsfjall, K: Krýsuvík, B: Brennisteinsfjöll, H: Hengill. Background topography is based on the IslandsDEM (Porter et al., 2018).

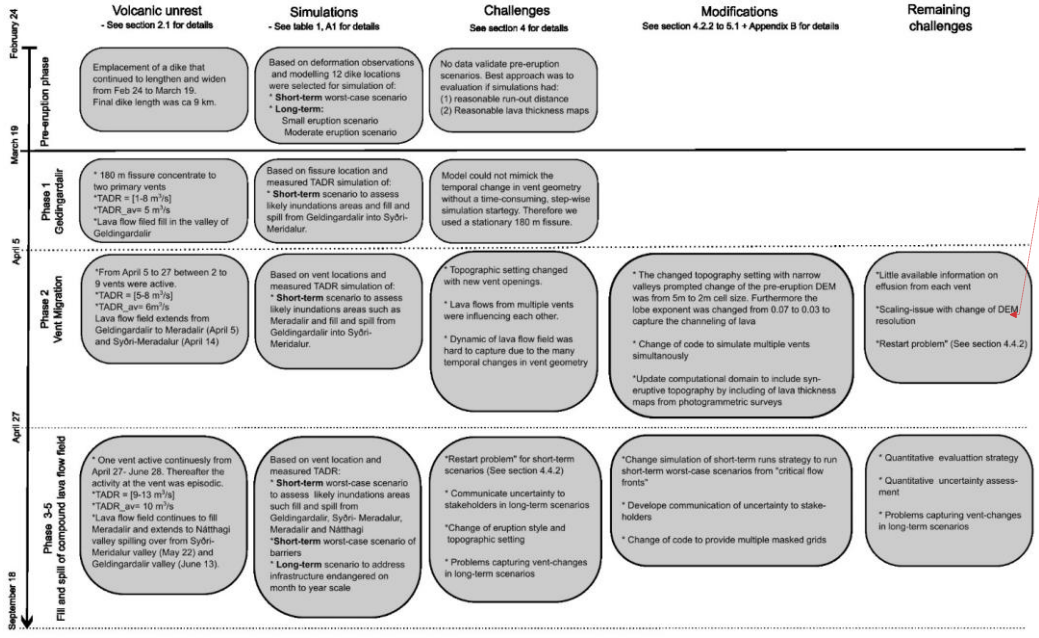

Figure 2: Illustration of the temporal development of the volcanic unrest (first column), the simulations performed addressing these developments (column 2), the identified simulation challenges (column 3), the modifications implemented to address these challenges (column 4) and the remaining challenges.

Formatted: Keep with next

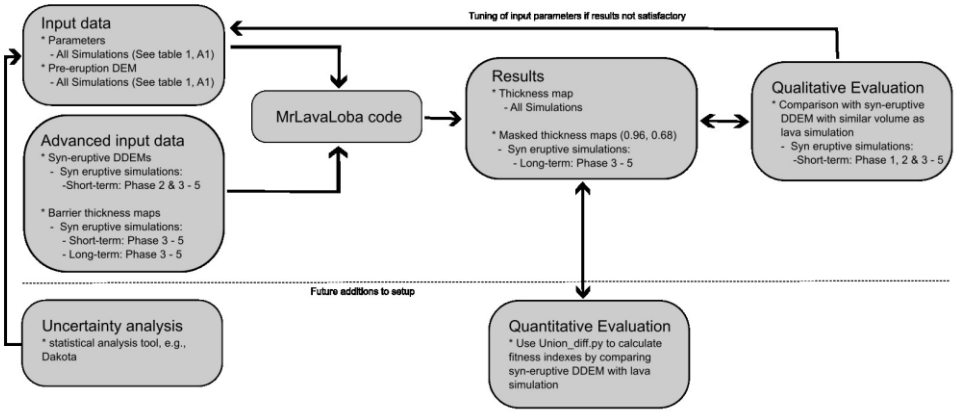

Figure 3: Flow chart for the lava flow simulations performed with the MrLavaLoba code during the Fagradalsfjall 2021 volcanic unrest. Suggested future improvements of the setup is added below the dashed line.

Formatted: Keep with next

Formatted: Left

Formatted: English (United Kingdom)

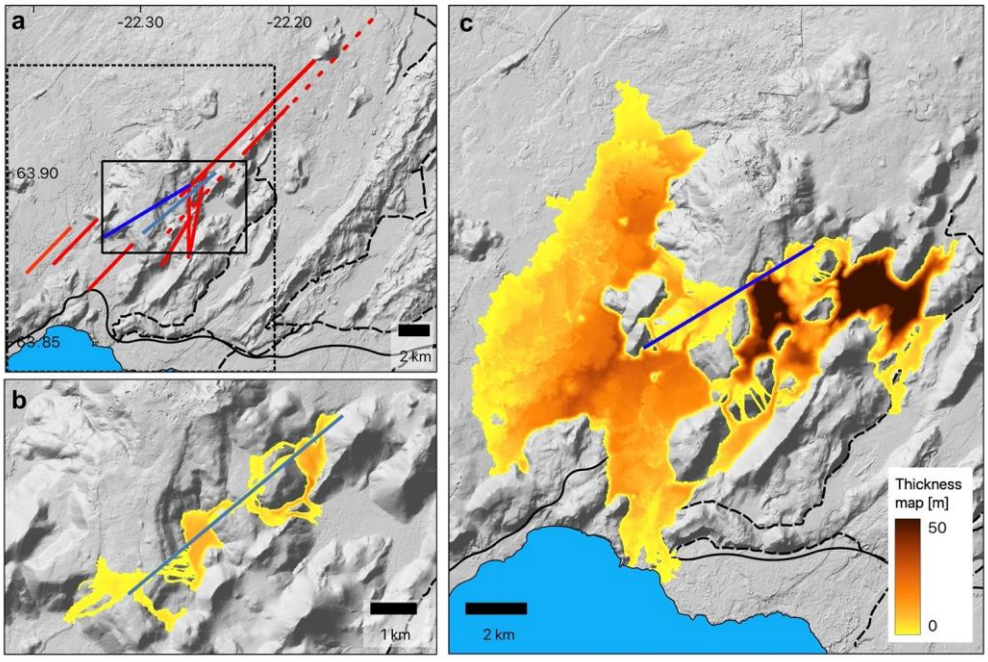

Figure 42: (a) Overview of modeled pre-eruption ~~modeled~~ potential fissures (red, light blue for fissure in frame b and dark blue for fissure in frame c). Solid black box indicates the extent of frame b and dashed black box indicates the extent of frame c. (b) Worst-case scenario (300 m^3/s) for t= 180 min for a pre-eruption fissure (~~dark~~ light blue). (c) Moderate scenario (0.3 km^3) run for a pre-eruption fissure (~~d~~darki~~ght~~ blue). Background topography is based on the IslandsDEM (Porter et al., 2018).

Formatted: Font color: Red

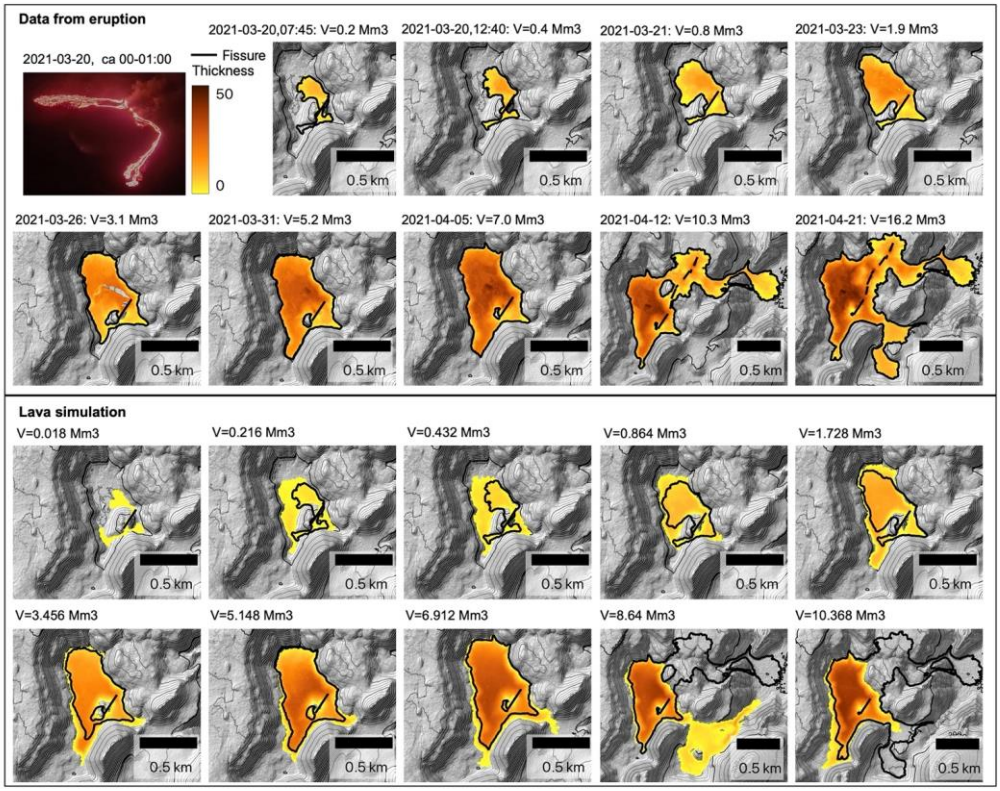

Figure ~~3~~5: Comparison between thickness maps obtained from the lava field (Upper box) in the first 24 days of the eruption (Pedersen et al., 2022b) and lava simulation thickness maps (Lower box). The volume of each thickness map is noted above each map. Thickness scale is the same for DDEMs and lava simulation thickness maps. The initial length of the first fissure is marked as a black line. The last two frames showing thickness maps from the eruption extend into phase 2 and therefore also include the fissures that opened ~~up~~ in ~~in~~ phase 2. Background topography is based on the IslandsDEM (Porter et al., 2018). Photo in the top left is by Freysteinn Sigmundsson.

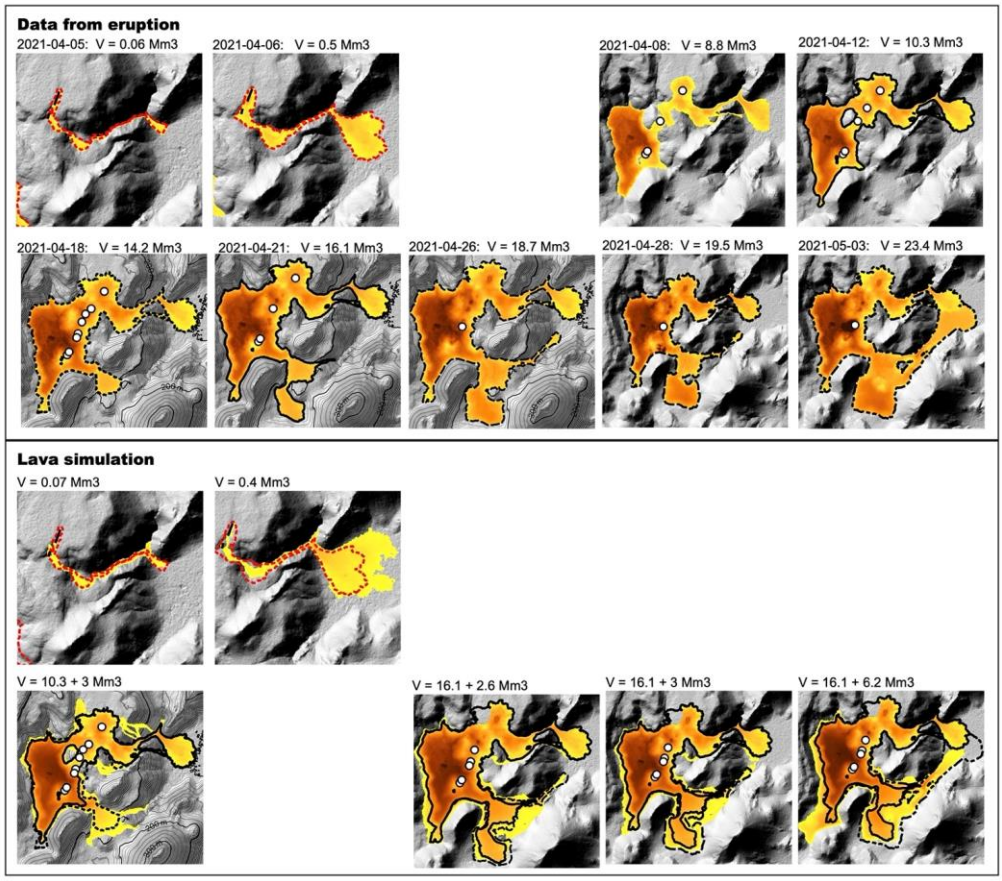

Figure 6: Comparison between thickness maps obtained from the lava field (Pedersen et al., 2022b) from April 5 to May 3 (Upper box) and lava simulation thickness maps performed during the vent migration phase (Lower box). The lava simulations in the bottom panel show the cumulative thickness of the syn-eruptive thickness map and the results from the simulation. The volume of each thickness map is noted above each map, which for the cumulative thickness maps is split into the volume contribution from the syn-eruptive thickness map and the simulation (e.g., V=16.1 + 6.2 Mm^3). The thickness scale is the same for DDEMs and lava simulation thickness maps going from 0 m (yellow) to 50 m (brown). The extent of the thickness maps used as input to the simulation has a solid black outline, while the extent of the lava thickness maps from the lava field with comparable volume is marked with hatched outlines. The active vents are in white, except for fissure 2 (top left), where the initial two fissure segments are shown as black lines. Background topography is based on the IslandsDEM (Porter et al., 2018).

Formatted: Superscript

~~Figure 4: Comparison between thickness maps obtained from the lava field (Pedersen et al., 2022b) from April 5 to May 3 (Upper box) and lava simulation thickness maps performed during the vent migration phase (Lower box). The lava simulations in the bottom panel show the cumulative thickness of the input thickness map and the results from the simulation. The extent of the thickness maps used as input to the simulation has a solid black outline, while the extent of the lava thickness maps from the lava field with comparable volume is marked with hatched outlines. The active vents are in white, except for the fissure 2, where the initial two fissure segments are shown as black lines. The full extent of the initial fissure segments was used to for the lava flow simulations. Background topography is based on the IslandsDEM (Porter et al., 2018).~~

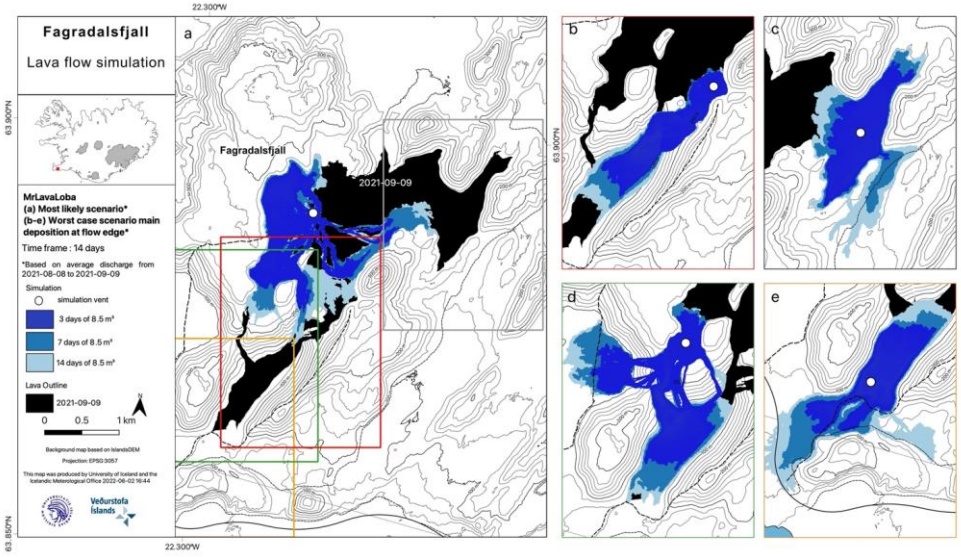

Figure 57: An example of how the short-term worst-case scenarios ~~from 9 September, 2021~~ were presented. Example from 9 September, 2021. (a) Simulation from vent 5, which was considered the most likely scenario. (b) ~~worst~~Worst-case scenario for Syðri-Meradalur to investigate if lava could exit the valley through the saddle point to the southeast. Based on these results the lava seemed more likely to exit south to Nátthagi. (c) ~~w~~Worst-case scenario for Meradalir to investigate if lava would spill to the east out of the valleys. Based on the results this was considered an option given the ~~vast~~ majority of erupted volume would reach Meradalir. (d) ~~worst~~Worst-case scenario for Geldingadalir to investigate if lava would spill to the southwest into Nátthag~~i~~a~~i~~kr~~i~~~~i~~k~~a~~i over the build barriers. Based on the results this was considered an option. (~~e~~e) ~~worst~~Worst-case scenario for Nátthagi to investigate if lava would spill to the south out of the valley. Based on the results this was considered an option given the ~~vast~~ majority of erupted volume would reach Nátthagi. Background topography is based on the IslandsDEM (Porter et al., 2018).

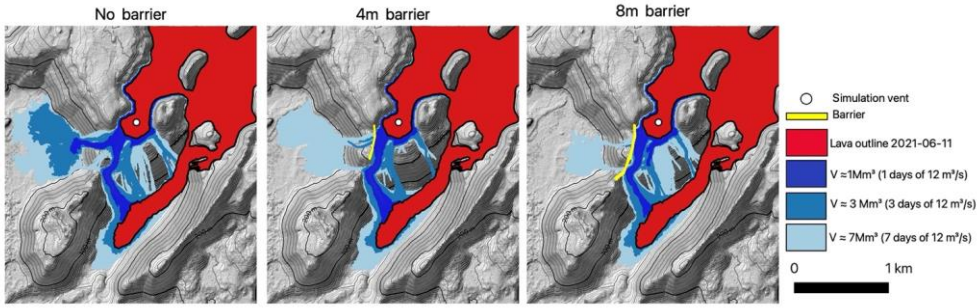

Figure ~~6~~8: An example of lava simulations predict ~~that~~ing how Geldingadalir would overflow with and without lava barriers. The simulation vent is located in southern Geldingadalir based on observation of lava inflation in ~~this~~ that area. Data based on survey from June 11, 2021 and the calculated volumes and time scales are based on the estimated TADR from ~~that~~ the same survey. Background topography is based on the IslandsDEM (Porter et al., 2018).

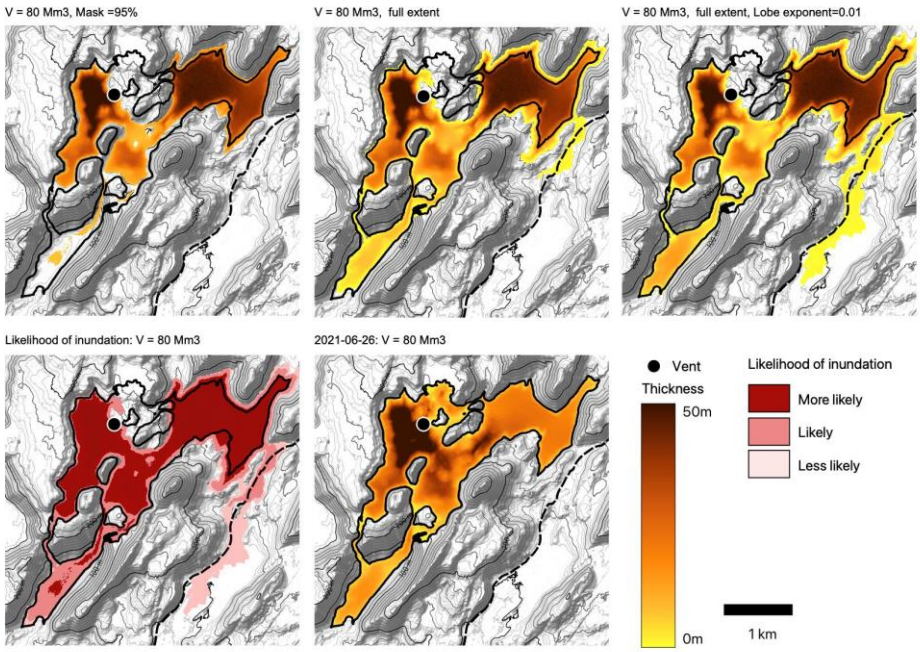

Figure 79: Top row: Example of the best tuning result for the 80 Mm3 simulation showing the 95 % lava thickness mask representing the category "More likely" and the full extent representing "Likely" category. To the right is a 80 Mm^3 simulation result with a lower lobe exponent, which representing the "Less likely" category. Bottom row: Map showing the likelihood of inundation based on the 80 Mm^3 simulations shown in the top row (Left) and lava thickness map from 2021-06-26 (Pedersen et al., 2022b), which can be compared to the simulation results in the top row (Right). Background topography is based on the IslandsDEM (Porter et al., 2018).

Formatted: Superscript

Formatted: Superscript

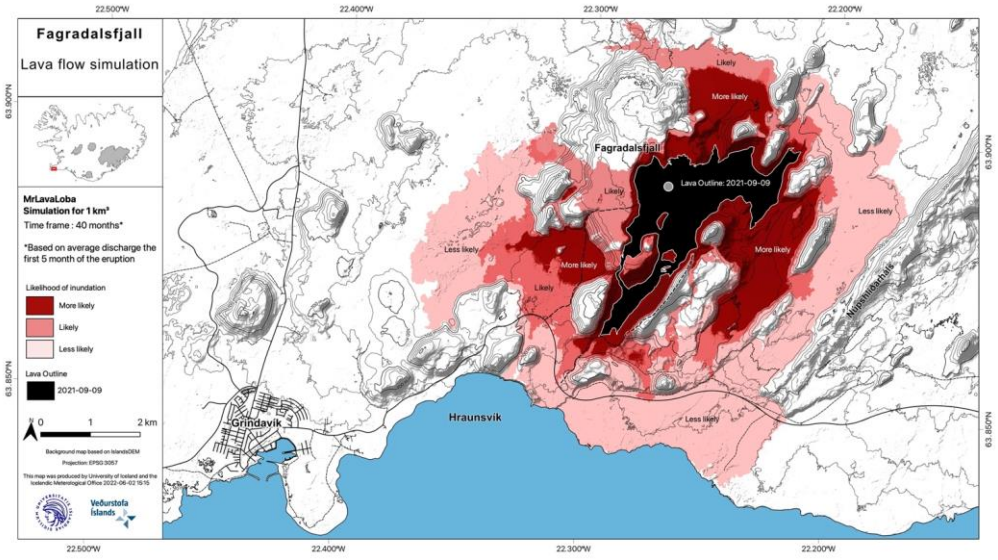

1200

Figure 8~~1~~10: Long-term scenario for lava emplacement of ~~a volume of~~ 1000 Mm^3 volume issued from vent 5. Background topography is based on the IslandsDEM (Porter et al., 2018).

Table 1 Overview of implementation strategies of MrLavaLoba for pre- and syn-eruptive simulations

	Pre-eruptive simulations			Syn-eruptive simulations			
	Short -term	**Longer-term**		**Short -term**			**Longer-term**
	Worst-case scenario	Small eruption scenario	Moderate eruption scenario	Phase 1: Geldingadalir	Phase ~~2:Vent~~2: Vent migration	Phase 3-5: Compound lava field	Phase 3-5: Compound lava field
Goal	Assess likely areas inundated hours after eruption start of high-effusion rate eruption	Gain insight to areas likely to be inundated within weeks from eruption start	Gain insight to areas likely to be inundated months after eruption start	Assess likely areas inundated first weeks of the eruption, including when Geldingadalir would spill into Syðri-Meradalur	Assess likely areas inundated during vent migration period, including when Geldingadalir would spill into Syðri-Meradalur	Forecast spilling of one valley to another. Evaluate areas endangered to lava inundation, specifically areas close to hiking paths/safety zones. Evaluate when barriers may be compromised	Address infrastructure endangered to lava flow inundation on month to year scale
Approach	Multiple runs with ~~with~~ various volumes simulating V= Q *x t, where Q= 300 m^3/s. Some of the input variables are made time-dependent	One run based on a pre-defined parameter space derived from scenarios compared with historical lava flows	One run based on a pre-defined parameter space derived from scenarios compared with historical lava flows	Multiple runs with ~~with~~ various volumes simulating V= Q *x t, where Q= TADR measurements from photogrammetric surveys. Some of the input variables are made ~~time-dependent~~time dependent.	Multiple runs with ~~with~~ various volumes simulating V= Q *x t, where Q= TADR measurements from photogrammetric surveys. Some of the input variables are made ~~time-dependent~~time dependent.	Multiple runs with ~~with~~ various volumes simulating V= Q *x t, where Q= TADR measurements from photogrammetric surveys. Some of the input variables are made time-dependent	Multiple runs with ~~with~~ various volumes () simulating V= Q*t, where Q= T~~T~~ADR_mean for the eruption~~.~~. All input parameters were tuned based on~~-~~ lava thickness maps obtained in June having volumes between 53-80 Mm^3
Evaluation	Lava run out length + lava thickness	Tuning compared to Illahraun (historical scenario)	Tuning compared to Arnaseturhraun (historical scenario)	Qualitative comparison to lava thickness maps	Qualitative comparison to lava thickness maps	NA	The eruption stopped at V= 150 Mm^3 and thus not comparable to our smallest long-term scenarios (250Mm^3)
DEM	Pre-eruption DEM (5 m x 5 m)	Pre-eruption DEM (10 m x 10 m)	Pre-eruption DEM (10 m x 10 m)	Pre-eruption DEM (5 m x 5 m)	Pre-eruption DEM (2 m x 2 m) / Pre-eruption DEM (5 m x 5 m) + DDEM from 2021-04-12 (5 m x 5 m) / Pre-eruption DEM (5 m x 5 m) + DDEM from 2021-04-21 (5 m x 5 m)	Pre-eruption DEM + newest thickness map + thickness map of lava barriers (if relevant)	Pre-eruption DEM (10 m x 10 m~~10 m x 10 m~~) + newest thickness map + thickness map of lava barriers (if relevant)
Vents	2/ 10 km fissures ~~selecated in the area of deformation~~(See Fig. 4a)	2/ 10 km fissures (See Fig. 4a)~~selecated in the area of deformation~~	2/ 10 km fissures (See Fig. 4a)~~selecated in the area of deformation~~	180 m fissure~~. Location and extent after the maximum opening observed in Geldingadalir~~	Fissure 2/All vents/ 5 southernmost vents	Vent 5/ Critical lava margins~~lava front edge at locations~~	Vent 5
Variable Parameters							

Formatted Table

Formatted: Superscript

Formatted: Superscript

Formatted: Superscript

Formatted: Superscript

Formatted: English (United States)

t [min]	30, 60, 180 ~~,~~ (360, 720)	NA	NA	t= V/ 10m3/s	t= V/ 5m3/s / t= V/ 8m3/s / t= V/ 5.1m3/s	3, 7, 14 days. ~~If 3 day scenario revealed inundation of areas close to hiking paths/safety zones~~Potentially 6 hr, 12 hr and 24 hr scenarios ~~would be modelled as well~~if needed.	t= V/ TADR_mean
Volume [m3]	300 m^3/s * t*60s	0.02	0.3	0 - 10 Mm^3	0 - 2.6 Mm^3 /0 - 3 Mm^3/ 0 - 6 Mm^3/	TADR m^3/s * t*60s	150 Mm^3, 250 Mm^3, 350Mm^3, 500 Mm^3, 1000Mm^3, 5000 Mm^3
n flows	150 per km fissure	400	1600	10	10 / 80/80	160	2000 / (3000 for >1000 M ~~k~~m^3)
minimum ~~n~~ lobes	3.33 ~~*~~ x t	400	1500	2 ~~*~~ x t[min]	2 ~~*~~ x t[min] / 2 ~~*~~ x t[min] / 1 ~~*~~ x t[min]	1 ~~*~~ x t [min]	3500
Lobe exponent	0.07	0.03	0.015	0.07	0.03/ 0.07/ 0.07	0.05	0.02 / 0.01

1205

Formatted: Superscript
Formatted: Superscript
Formatted: Superscript
Formatted: Superscript
Formatted: Superscript
Formatted: Superscript
Formatted: Superscript
Formatted: Superscript
Formatted: Superscript
Formatted: Superscript
Formatted: Superscript
Formatted: Superscript
Formatted: Superscript

Table 2: Overview of advantages and disadvantages of the MrLavaLoba code

MrLavaLoba code	
Advantages	**Disadvantages**
• Free ~~&~~and easy to run in python • Very flexible and can be used for various simulation purposes • Fast computational time • Can run very large scenarios • Change topography during model run • Produce lava thickness layer • Includes volume + final extent • Can be used to assess infilling of depressions, valleys and overflows of barriers • Can handle multiple vents • Easy to implement barriers & new topography/thickness layer	• ~~Not a physical model: i~~Input parameters have to be tuned to: known scenarios~~;~~, individual eruptions~~;~~, ~~specifics~~specific to type of activity~~;~~ and different topographic setting~~.~~ • Do not provide time/velocity evolution of lava emplacement in a single run • Do only mimic channel/tube formation if tuned for that,- does not develop inherently in the model • Do not include vent processes→ underestimate thickness of deposits close to the vent (thus DDEM should be implemented to account for that) • Results not designed for hazard communication

Formatted: Space After: 0 pt, Border: Top: (No border), Bottom: (No border), Left: (No border), Right: (No border) Between : (No border)

Appendix A

Table A1: Overview of all input parameters used depending on modelling approach. M: 1000000, t: time

Tuning Parameters	Pre-eruptive simulations			Syn-eruptive simulations			
	Short -term	Longer-term		Short -term			Longer-term
	Worst-case scenario: 300 m3/s	Small eruption scenario	Moderate eruption scenario	Phase 1: Geldingardalir	Phase 2:Vent migration	Phase 3-5: Compound lava field	Phase 3-5: Compound lava field
source DEM [in EPSG 3057]	Pre-eruption DEM (5 m -x 5 m)	Pre-eruption DEM (10 m- x 10 m)	Pre-eruption DEM (10 m -x 10 m)	Pre-eruption DEM (5 m x 5 m)	Pre-eruption DEM (2 m x 2 m)/ Pre-eruption DEM (5 m x 5 m) + DDEM from 2021-04-12 (5 m x 5 m) / Pre-eruption DEM (5 m x 5 m) + DDEM from 2021-04-21 (5 m x 5 m)	Pre-eruption DEM + newest thickness map + thickness map of lava barriers (if relevant)	Pre-eruption DEM (10 ~~m x~~m x 10 m) + newest thickness map + thickness map of lava barriers (if relevant)
vent_flag	2	2	2	2	~~8~~7	~~8~~7	~~8~~7
x_vent [in EPSG 3057]	[x1, x2] 2/ 10 km fissures (See Fig. 4a)	[x1, x2] 2/ 10 km fissures (See Fig. 4a)	[x1, x2] 2/ 10 km fissures (See Fig. 4a)	[339326 ,339423]	Combination of following vents: [339366, 339386, 339522, 339489, 339467, 339473, 339545]	[339048]	[339048]
y_vent [in EPSG 3057]	[y1, y2] 2/ 10 km fissures (See Fig. 4a)	[y1, y2] 2/ 10 km fissures (See Fig. 4a)	[y1, y2] 2/ 10 km fissures (See Fig. 4a)	[380202 ,380364]	Combination of following vents: [380288, 380319, 380637, 380515, 380471, 380440, 380695]	[380058]	[380058]
hazard_flag	1	1	1	1	1	1	1
fissure_probabilities	NA	NA	NA	NA	[1, 1, 1, 5, 5, 5, 1]	[1]	[1]
masking_threshold	0.96	0.96	0.96	0.96	0.96	[0.68 ,0.96]	0.95
n_flows	150 per km fissure	400	1600	10	10 / 80/80	160	1000
min_n_lobes	3.33 x* t[min]	400	1500	2 * x t[min]	2 * x t[min] / 2 * x t[min] / 1 * x t[min]	1* x t [min]	3500
max_n_lobes	min_n_lobes	min_n_lobes	min_n_lobes	min_n_lobes	min_n_lobes	min_n_lobes	min_n_lobes
volume_flag	1	1	1	1	1	1	1
total_volume	300 m^3/s * x t[s]~~time~~	20M~~000000~~	300M~~000000~~	TADR [m^3/s] * x t[s]	TADR [m^3/s] * x t[s]	TADR [m^3/s] * x t[s]	150 M, 250 M, 350M, 500 M, 1000M, 5000M
fixed_dimension_flag	1	1	1	1	1	1	1
lobe_area	250	1000	1000	250	250	250	1000
thickness_ratio	0.9	2	2	0.9	0.9	0.9	2
topo_mod_flag	2	2	2	2	2	2	2
n_flows_counter	1	1	1	1	1	1	1

Formatted: Superscript

Formatted: Superscript

Formatted: Superscript

Formatted: Superscript

n_lobes_counter	1	1	1	1	1	1	1
thickening_parameter	0.06	0.06	0.06	0.06	0.06	0.06	0.02
lobe_exponent	0.07	0.03	0.015	0.07	0.07	0.05	0.02
max_slope_prob	0.8	0.8	0.8	0.8	0.8	0.8	0.8
inertial_exponent	0.1	0.1	0.1	0.1	0.1	0.1	0.1

Appendix B

In this appendix we describe the modifications implemented in the code MrLavaLoba to improve its usage during and after the 2021 Fagradalsfjall eruption. These changes have been uploaded to the MrLavaLoba Github repository (https://github.com/demichie/MrLavaLoba) as commits, which are records with unique ID, that identifies specific changes in github documents, when the changes were made and who made them. The code that has been added is highlighted in green, while code that has been deleted is in red.

1) April 2021 (commit 9f60549): Simulation of the whole ongoing eruption as a series of "phases".
This commit improved the usage of restart files, i.e. the possibility to start a new simulation including the output of a previous simulation. After this change the code allows to implement the simulation of the eruption as a series of "phases" without losing the benefit of the thickening parameter.

2) April 2021 (commits 80d4230, e2885d1, 9e1826c,23f6a16, 2311a50): Possibility to have multiple vents/fissures.

These commits enabled implementation of the possibility to consider multiple fissures/vents and to assign different probability to be active to each fissure. Here there is a list of the new conditions available:

- vent_flag = 4 => the initial lobes are on multiple fissures and all points of the fissures have the same probability that a “lobe chain” will start from them
- vent_flag = 5 => the initial lobes are on multiple fissures and all the fissures have the same probability that a “lobe chain” will start from them
- vent_flag = 7 => the initial lobes are on multiple fissures and the probability of each fissure is fixed by "fissure_probabilities"

3) September 2021 (commit 3c4e5d3): Enable multiple threshold values.

In addition to the final lava thickness map, the MrLavaLoba code allows saving masked grids obtained by considering inundated cells fulfilling a specified threshold value (de’ Michieli Vitturi and Tarquini, 2017). This is controlled by the input parameter masking_threshold, expressed in fraction of the total volume (i.e. varying within the interval [0; 1]). As an example, if the cut is applied to the thickness and masking_threshold is set to 0.95, the thinnest portion of the final lava deposit representing 5% of the total volume emplaced is cut out from the results. In the original version of MrLavaLoba it was possible to set a single value of masking_threshold for each simulation, but with this commit it is possible to set multiple values and thus save multiple output raster files.

4) January 2022 (commits d6d0953, 08afee3): code optimization.

With these commits input parameters to crop the DEM file, and then the computational domain, have been introduced. This crop reduces the computational time when the DEM is large and the area covered by the flow is a lot smaller.
In addition, an analysis with a profiler identified the numpy function “copy”, used to create a copy of a Numpy array, which was a bottleneck of the code. For this reason, the code has been rewritten to reduce the call to this function. The two changes increased the speed of the code by a factor of 5 to 10. The optimization also allowed us to remove some input parameters that became unnecessary after the changes.